

Title: Distribution and biophysical processes of beaded streams in Arctic permafrost landscapes

Authors: Arp, Whitman, Jones, Grosse, Gaglioti, and Heim

### Abstract

Beaded streams are widespread in permafrost regions and are considered a common thermokarst landform. However, little is known about their distribution, how and under what conditions they form, and how their intriguing morphology translates to ecosystem functions and habitat. Here we report on a Circum-Arctic survey of beaded streams and a watershed-scale analysis in northern Alaska using remote sensing and field studies. We mapped over 400 channel networks with beaded morphology throughout the continuous permafrost zone of northern Alaska, Canada, and Russia and found the highest abundance associated with medium- to high- ground-ice content permafrost in moderately sloping terrain. In one Arctic Coastal Plain watershed, beaded streams accounted for half of the drainage density, occurring primarily as low-order channels initiating from lakes and drained lake basins. Beaded streams predictably transition to alluvial channels with increasing drainage area and decreasing channel slope, although this transition is modified by local controls on water and sediment delivery. Comparison of one beaded channel using repeat photography between 1948 and 2013 indicate a relatively stable landform and  $^{14}\text{C}$  dating of basal sediments suggest channel formation may be as early as the Pleistocene-Holocene transition. Contemporary processes, such as deep snow accumulation in riparian zones effectively insulates channel ice and allows for perennial liquid water below most beaded stream pools. Because of this, mean annual temperatures in pool beds are greater than  $2^{\circ}\text{C}$ , leading to the development of perennial thaw bulbs or taliks underlying these thermokarst features that range from 0.7 to 1.6 m. In the summer, some pools thermally stratify, which reduces permafrost thaw and maintains coldwater habitats. Snowmelt generated peak-flows decrease rapidly by two or more orders of magnitude to summer low flows with slow reach-scale velocity distributions ranging from 0.01 to 0.1 m/s, yet channel runs still move water rapidly between pools. The repeating spatial pattern associated with beaded stream morphology and hydrological dynamics may provide abundant and optimal foraging habitat for fish. Beaded streams may create important ecosystem functions and habitat in many permafrost landscapes and their distribution and dynamics are only beginning to be recognized in Arctic research.

## 1 **1 Introduction**

2 Channels with regularly spaced deep and elliptical pools connected by narrow runs are a common  
3 form of many streams that drain Arctic permafrost foothills and lowlands. These channels are  
4 often referred to as “beaded” streams because during summer low flows, pools appear as *beads-*  
5 *on-a-string* of runs (Oswood et al., 1989). Beaded streams are generally treated in scientific  
6 textbooks on permafrost (e.g., Davis, 2001), hydrology (e.g., Woo, 2012), and aquatic ecology  
7 (e.g., McKnight et al. 2008), yet to our knowledge field investigations of these systems has been  
8 limited to Imnaviat Creek in northern Alaska (e.g., Oswood et al., 1989) and the Yamal Peninsula  
9 in Siberia (Tarbeeva and Surkov, 2013).

10 Our understanding of the physical and chemical character of beaded streams mainly comes  
11 from Imnavait Creek in the Arctic Foothills of Alaska (Oswood et al., 1989). Subsequent studies  
12 of this and adjacent systems suggest how beaded morphology functions in permafrost thaw  
13 (Brosten et al., 2006), hydrologic storage and hyporheic exchange (Merck et al., 2012; Zarnetske  
14 et al., 2007), and thermal regimes (Merck and Neilson, 2012). Thermal stratification in pools up  
15 to 2-m deep often occurs in beaded channels during summer low flows (Oswood et al., 1989) and  
16 this may play a role in permafrost thaw, hydrologic transport, and nutrient processing as the  
17 Arctic climate changes (Zarnetske et al., 2008; Merck and Neilson, 2012). In the winter, foothill  
18 streams freeze solid (Best et al., 2005) such that bed sediments thaw slowly and to a limited depth  
19 compared to adjacent alluvial channels (Brosten et al., 2006; Zarnetske et al., 2007). Winter  
20 analysis of multiple aquatic habitats on the Arctic Coastal Plain (ACP), however, shows that  
21 beaded streams can maintain liquid water under ice and potentially develop perennially thawed  
22 sediments (Jones et al., 2013). These physical regimes of water and energy flow in Arctic  
23 streams, coupled with channel morphology and drainage network organization likely also dictate  
24 how these ecosystems function as aquatic habitat (Craig and McCart, 1975). Hydrographic  
25 analysis of the Fish Creek Watershed on the ACP show that beaded streams form the dominant  
26 connections between larger river systems and abundant thermokarst lakes, thus influencing both  
27 hydrology and the movement of aquatic organisms between habitats (Arp et al. 2012b).

28 Beaded streams are thought to be a common Arctic thermokarst landform and occur mainly  
29 in association with ice-wedge networks of polygonized tundra (Pewé, 1966). The formation of

30 channel drainage in these streams occurs along ice-wedge troughs with mature drainage channels  
31 resulting in complete degradation of ice wedges by thermal erosion (Lachenbruch, 1966).  
32 Classification of Arctic streams place beaded channels within the *tundra* class as compared to  
33 *springs* and *mountain* classes (Craig and McCart, 1975). In foothills watersheds, beaded streams  
34 are typically fed by linear hillslope water tracks (McNamara et al., 1999), while on the ACP these  
35 channels initiate mainly from thermokarst lakes and drained thermokarst lake basins (DTLBs)  
36 (Arp et al., 2012b; Whitman et al., 2011). Based on existing research, it is uncertain whether high  
37 densities of beaded streams exist beyond this long-standing focal site (Imnavait Creek / Toolik  
38 Lake) and this more recent studied watershed (Fish Creek). Newly published work from Russian  
39 permafrost zones is also expanding our knowledge of beaded stream distribution (Tarbeeva and  
40 Surkov, 2013). Still, an understanding of their formative processes and the broader watershed  
41 functions they provide are currently lacking.

42           Knowing where beaded streams occur in permafrost landscapes and how these fluvial  
43 forms are organized within drainage networks will help advance our understanding of their  
44 broader role in watershed, ecosystem, and biological functions across the Arctic. Such analyses  
45 will also help in predicting changes in these thermokarst fluvial systems with respect to climate  
46 and land-use changes and corresponding permafrost responses and hydrologic feedbacks. In this  
47 study, we (1) describe the distribution of beaded streams from Circum-Arctic to regional scales,  
48 (2) explore whether the distribution and variation in beaded morphology helps explain physical  
49 functioning, the evolution of beaded streams, and their responsiveness to external drivers, and 3)  
50 highlight the important role that these ecosystems serve in aquatic habitat. This work expands our  
51 understanding of beaded streams beyond the foothill regions of Arctic Alaska where most all  
52 previous work has been completed, both in terms of fundamental aspects of permafrost and  
53 fluvial processes as well as aspects relevant to fish and other aquatic biota.

54

## 55 **2 Methods**

### 56 **2.1 Study areas, distribution surveys, and classification**

57 The distribution and abundance of beaded streams were determined by using a nested survey  
58 design and a range of survey methods. These nested domains ranged from a 1) Circum-Arctic  
59 assessment confined to the zone of continuous permafrost using imagery in Google Earth (GE)  
60 (Table 1 and Fig. 1), 2) aerial transects across landscape gradients on the North Slope of Alaska  
61 (Fig. 2), and 3) a census of the Fish Creek Watershed (4700 km<sup>2</sup>) using high resolution  
62 photography (Fig. 3). We also conducted field studies throughout this watershed and used data  
63 from an ongoing monitoring network at several streams in the lower portion the watershed to  
64 characterize biophysical processes and habitat.

65 The Circum-Arctic survey utilized imagery available in GE to identify channels with beaded  
66 morphology. This analysis focused on the continuous permafrost zone north of 66° latitude. We  
67 utilized the historical image browser function in GE to access the highest resolution imagery (<  
68 5-m) possible for a given region. This analysis focused on portions of Alaska (U.S.A.), Siberia  
69 (Russia), and northern Canada totaling approximately 4.5 million km<sup>2</sup>. We found that most  
70 channels with beaded morphology could be identified when scanning images at 1:6,000 when the  
71 imagery had a resolution of 5-m or finer and was mostly snow-free. The availability of high  
72 resolution, snow-free imagery in Alaska was quite good, covering 80% of the continuous  
73 permafrost zone surveyed. In Russia and Canada, the availability of such imagery was much  
74 lower, 11% and 9%, respectively, as of 2013 (Table 1). Prospective beaded channels recognized  
75 while scanning were inspected more closely (finer scale) to verify their form and the course was  
76 marked as the furthest downstream network point of the continuous beaded channel. Surface  
77 elevation, latitude, and classes of permafrost ground ice were attributed to each point using  
78 thematic datasets for panarctic (Brown et al., 1998) and Alaska-focused permafrost and ground  
79 ice distribution (Jorgenson et al., 2008) and surface elevation. In order to compare among regions  
80 with differing extents of sufficient imagery, we extrapolated the number of surveyed streams  
81 based on the proportion of high resolution imagery available to estimate the total number of  
82 beaded stream networks in the Circum-Arctic continuous permafrost zone (Table 1). We  
83 additionally estimated drainage density of beaded channels based on assuming an average  
84 network length of 10 km, which results in only a broad regional average and definitely varies  
85 considerably on finer scales.

86 Regionally (Alaska North Slope) focused aerial surveys in a Cessna 185 were flown on 10  
87 July 2011 on a clear day along three transects. One 270 km transect was from the Brooks Range  
88 divide north to the Colville River Delta, which moves from glaciated terrain in the upper foothills  
89 to vast areas north of the Pleistocene Glacial Maximum (Fig. 3). Another transect was 130 km  
90 from Prudhoe Bay to the lower Fish Creek Watershed on the Arctic Coastal Plain (ACP), and a  
91 third transect spanned 36 km of land area from Fish Creek to the lands north of Teshekpuk Lake  
92 representing an inner to outer ACP gradient. During the transect flights at approximately 150 m  
93 elevation, one observer had a sufficient view of approximately 500 m land surface to one side of  
94 the plane, thus covering approximately 220 km<sup>2</sup> of land surface in these surveys. During the flight  
95 each stream observed was marked with a GPS, photographed, and later these photographs were  
96 inspected to determine which streams could be classified as having beaded morphology.

97 The watershed census of beaded streams was conducted in the Fish Creek Watershed as part  
98 of a broader effort to map, classify, and understand watershed hydrography and its role in  
99 watershed runoff processes (Arp et al., 2012b). The Fish Creek Watershed is located in the  
100 northeastern portion of the National Petroleum Reserve – Alaska (NPR-A) on the ACP (Figs. 3).  
101 Surface deposits grade from marine-alluvial silt with some pebbly substrates in the east to  
102 inactive eolian sand dune fields in the west (Carter, 1981; Carter and Galloway, 2005). The sand-  
103 bedded alluvial rivers, Fish Creek (*Ulutuuq*, Inupiat name) and its tributary Judy Creek  
104 (*Iqalliqpiq*), drain this area and form a delta in the Beaufort Sea just west of the Colville River  
105 Delta. Both rivers begin as beaded streams, Judy in a narrow arm extending into the foothills and  
106 Fish in the sand sea. The Ublutuooh River (*Tingmiaqsiiuvik*) also starts as a beaded stream, but  
107 maintains this morphology for a longer distance before becoming a gravel-bedded alluvial  
108 channel near its confluence with Fish Creek (Fig. 3). All perennial channels in the Fish Creek  
109 Watershed were delineated from 2002 mid-July color infrared (CIR) photography (2.5-m  
110 resolution) in a GIS environment. Streams with beaded morphology were quantified according  
111 pool density and size (measured as width perpendicular to the direction of flow) and valley  
112 gradient from a 5-m interferometric synthetic aperture radar (IfSAR) digital elevation model  
113 (DEM) at a segment scale, typically 1-3 km length that was representative of individual drainage  
114 networks. These segments were also placed into four classes according to predominant pool  
115 (channel bead) shape and connectivity to runs as: 1) elliptical (round) pools separated by distinct

116 connecting runs (Fig. 4b), 2) coalesced pools (elliptical pools merged together) without distinct  
117 connecting runs (Fig. 4c), 3) large irregularly shaped pools often connected by long runs (Fig. 4d,  
118 and 4) connected thaw pits in degrading polygonized tundra connected by perennial or ephemeral  
119 streams (Fig. 4e). We used this classification to help evaluate if pool form of beaded morphology  
120 was correlated with landscape position within the watershed and permafrost ice-content or other  
121 thermokarst landforms (e.g., thermokarst lakes and DTLBs). We visited approximately 20% of  
122 these stream channels in the Fish Creek Watershed during late July 2011 to verify beaded  
123 morphology and classification and to collect additional field measurements, as described below in  
124 the next section.

125

## 126 **2.2 Geospatial and field measurements**

127 A subset of stream channels mapped and classified in the Fish Creek Watershed (Arp et al.,  
128 2012b) were used for detailed geomorphic and hydrologic analysis in this study. Specifically, we  
129 targeted a set of each channel class representing beaded streams and alluvial channels (Fig. 4), as  
130 well as points of channel initiation. During field visits, we measured stream discharge using the  
131 velocity-area method. Along stream reaches equaling 20 or more channel widths (typically 100 –  
132 300 m), we surveyed the water surface elevation at 5-7 points with an engineer's level, stadia rod,  
133 and tape to measure the channel slope. At the same time, channel cross-sections that bisected  
134 pools were surveyed at 2-3 locations to measure pool geometry as well as the incised zone  
135 surrounding the channel (gulch) indicated by riparian vegetation and form.

136 In order to better understand controls on beaded stream morphology, we conducted similar  
137 surveys in the field, and from geospatial data (CIR photography and DEMs) along a longitudinal  
138 gradient of Fish Creek and the Ublutuoch River from their headwaters downstream (Fig. 3). For  
139 each fluvial system, at least three reaches were studied in the field where the channel had  
140 distinctly beaded form and three reaches were studied downstream where the channel had  
141 transitioned to an alluvial form. Additional locations were later selected to better refine this  
142 transition including identification of sediment sinks (flow-through lakes) or clear-water inputs  
143 (lake-fed tributaries) relative to potential sediment sources including contact points with  
144 hillslopes and sand dunes, and tributaries originating from DTLBs or upland tundra. Such local

145 controls on delivery of new water and sediment to channels were expected to help explain  
146 changes in form downstream, similar in concept to mountain drainage networks flowing through  
147 lakes (Arp et al. 2007) and as hypothesized for Arctic drainage networks (Tarbeeva and Surkov,  
148 2013). The total length of channels analyzed for the Fish Creek Watershed was about 135 km and  
149 the total length of channels analyzed for the Ublutuoch River Watershed was about 70 km.

150

### 151 **2.3 Analysis of channel change and history**

152 To better understand the evolution of beaded channels we compared the position and morphology  
153 of one channel over a 64 year period using high resolution (1:24,000 scale) photography from  
154 1948 (Black and White, Naval Arctic Research Laboratory (BW NARL)) and 2013 (color-  
155 infrared at 25-cm pixel size, Aerometric Inc) located in the Fish Creek Watershed. This was done  
156 to examine the hypothesis that beaded streams evolve in a manner similar to observed  
157 degradation of ice-wedge intersections, but lacking channel connectivity. The 1948 BW NARL  
158 photographs were acquired from the University of Alaska Fairbanks GeoData Center and scanned  
159 at 1200 dpi. The scanned images were georeferenced with 20 ground control points (primarily,  
160 stable ice-wedge intersections) to a light detection and ranging (LiDAR) dataset (detailed below)  
161 using a spline transformation and converted to a pixel-size of 0.5 m. The 2013 color photography  
162 was acquired, by Aerometric, Inc. on 4-September to complement airborne LiDAR data. Manual  
163 analysis of both datasets was conducted in black and white to avoid any bias that may have arisen  
164 due to differences in film types and their separation by so many years of time. Particular  
165 attention was given to any changes in channel form (location and plan-view dimensions) relative  
166 to ambient polygonized tundra within a 100-m buffer of the channel and the presence and  
167 dynamics of thaw pits. All stream channels in both images were independently delineated  
168 manually and individual pools and ice-wedge intersections with pits marked with a central point.  
169 We tracked individual pools (beads) and thaw-pits from 1948 to 2013 and also recorded those  
170 features that were observed in one time period but not the other. The channel gulch / riparian  
171 corridor was also delineated for both periods, based primarily on the darker (greener) signature of  
172 taller sedges, willows, and dwarf birch and moister understory bryophyte communities.

173 In order to estimate the timing of pool initiation, long-term sedimentation rates, and the  
174 depositional environment of pools, we collected sediment cores to analyze sediment stratigraphy  
175 and estimate age-depth relationships using  $^{14}\text{C}$  dating. In April 2012, two overlapping cores were  
176 collected from a large, deep pool in Crea Creek (Fig. 3) to a depth of 75 cm (base of unfrozen  
177 talik) using a Russian Peat Corer. Each core was photographed and subsampled at 5-cm  
178 increments with subsamples placed in Whirl-Pak<sup>TM</sup> bags. Here we identified what appeared to be  
179 basal sediments where the channel initiated, as indicated by an organic sediment layer with  
180 fibrous terrestrial organic remains sitting above a homogenous and thick sand layer extending  
181 down into the base of the talik. We sampled an individual twig from this basal section for  $^{14}\text{C}$   
182 dating. Several moss and sedge samples were also collected from above the basal layer in organic  
183 rich, sandy sediments, similar to organic-rich *gyttja* deposited in lakes of the region, for dating as  
184 well. Another core was collected from a pool in 2013 at nearby Blackfish Creek (Fig. 3) and  
185 macrofossils were collected from above several distinct sand horizons within the core. The plant  
186 macrofossils were prepared for analysis with an acid-base treatment and analyzed for  $^{14}\text{C}$  content  
187 using standard acceleratory mass spectrometry techniques at the NOSAMS facility at Woods  
188 Hole Oceanographic Institute. All radiocarbon dates were calibrated to calendar ages using the  
189 Intcal 13 curve (Reimer et al., 2013) and are reported as the mean and two-sigma ranges of the  
190 calibrated ages.

191

## 192 **2.4 Hydrologic monitoring and habitat analysis**

193 As part of an on-going monitoring program (Fish Creek Watershed Observatory; Whitman et al.,  
194 2011), streamflow, water temperature, and other water quality parameters have been recorded at  
195 hourly intervals at five stream-lake systems since 2008. These small catchments (Fig. 3) are  
196 being monitored by the Bureau of Land Management (BLM) Arctic Field Office to collect  
197 baseline data prior to expected changes in land use, primarily new oil development, and  
198 associated lake-water extraction for ice road construction and facility operations in the NE NPR-  
199 A. Stream gauging was conducted using autonomous pressure transducers (Onset U20-001-01)  
200 anchored to pool beds, which were corrected to local atmospheric pressure to measure water  
201 height. Stream discharge was measured using the velocity-area method with either an ADCP



202 (Flowtracker™) or electromagnetic (Hach™) velocity meter mounted to a top-setting wading  
203 rod. Approximately 20 velocity measurements were made per cross-section at increments spaced  
204 to not exceed 10% of total discharge. Typically we made 3-4 measurements near the snowmelt  
205 peakflow in early to mid-June, 2-3 measurements during peakflow recession in late June or early  
206 July and 2-3 measurements again in late July and late August. Rating curves were fit with a log or  
207 power law equation to estimate continuous discharge during the ice-free season; separate high-  
208 flow and low-flow rating curves were often required. Based on temperature sensors placed in  
209 channel runs and comparison with time-lapse cameras set during several years, we assumed that  
210 streamflow ceased during October in most years.

211 We tested how contrasting beaded stream morphometry and watershed features affected  
212 hydrologic residence times and velocity distributions using tracer tests on two stream reaches  
213 with contrasting morphology and flow regimes (Fig. 6). At Crea and Blackfish creeks (Fig. 3),  
214 we identified 325-m and 232-m reaches, respectively, starting and ending at channel runs to  
215 ensure initial mixing and sampling of the advective flow. Rhodamine WT (RWT), a pink  
216 fluorescent dye, was used as a water tracer because it can be detected at low concentrations and  
217 only small quantities are required to reach target concentrations, which is an important practical  
218 consideration for remote field sites. RWT has low biological reactivity, yet does sorb to organic  
219 matter and begins photodegrading after several days of sunlight exposure at low concentrations  
220 (Vasudevan et al., 2001). Thus, RWT is not truly conservative, however is widely use to  
221 characterize channel hydraulics and transient storage processes, including previous work in  
222 Arctic beaded streams (Zarnetske et al. 2007). Based on targeted downstream peak  
223 concentrations of 30 ppb, we made pulse additions of RWT at reach heads and monitored  
224 concentration at the reach bottom using a YSI 6600-V2 water quality sonde with a RWT probe.  
225 This experiment typically lasted a day or longer to account for all tracer moving through the  
226 system. RWT tracer data were then fit with the model One-dimensional Transport model with In-  
227 channel Storage and Parameterization (OTIS-P) to estimate advective channel area (A), storage  
228 zone area (A<sub>s</sub>), dispersion (D), and the storage exchange coefficient ( $\alpha$ ) (Runkel, 2000). Percent  
229 RWT recovery averaged 81% with an average sorption coefficient ( $\lambda$ ) of  $1 \times 10^{-5}$  used to account  
230 for this loss downstream. Tracer breakthrough curve data was plotted as cumulative solute  
231 recovered downstream and converted to velocity distribution by dividing reach length by travel

232 time. RWT injections were conducted at both Crea and Blackfish creeks in mid-June near  
233 peakflows, in early July (late peakflow recession), and late August (low summer baseflow).

234 Stream thermal regimes were quantified using the same pressure transducers anchored to  
235 pool beds that also record temperature, along with thermistors (Onset U12-015) near the surface  
236 of pools (30-cm below) and in channel runs of each beaded stream; all recording at hourly  
237 intervals. These paired temperature measurements were used to assess thermal regimes and  
238 timing and extent of stratification in pools assuming that a ratio of surface temperature to bed  
239 temperature  $>1.1$  indicated stratification. Using this system, one pool and corresponding channel  
240 run have been monitored among five streams year-round from 2009-2013 (Fig. 3). To assess  
241 variability in thermal regimes and particularly stratification within stream systems, we selected an  
242 additional three pools of varying depth and area in both Crea and Blackfish creeks (Fig. 3) in  
243 2012 and instrumented these with additional bed and surface thermistors. These were retrieved  
244 and downloaded in late August 2013.

245 During the late winters (March and April) of 2010-2013, we visited several of these same  
246 beaded stream reaches concurrent with lake-ice, snow, and water chemistry surveys. When  
247 opportunities existed, we measured snow depth either with a 3-m avalanche probe or by digging a  
248 pit, or both, above frozen pools located with a GPS. Holes were augered through the ice and ice  
249 thickness and below-ice water depth was measured using an ice-thickness gauge (Kovacs  
250 Enterprises LCC™). We also measured the depth of thawed sediment (talik) using multiple 1.2-m  
251 threaded stainless steel rods fitted with a blunt tip and driven with a slide-hammer to the depth of  
252 refusal (typically 10-20 pounds with no downward movement). When possible these late winter  
253 surveys were done repeatedly at the same pools including measurements of dissolved oxygen,  
254 specific conductance, and pH to assess the quality of overwintering fish habitat.

255

256

## 257 **3 Results and Discussion**

### 258 **3.1 Beaded stream distribution**

259 Using available high-resolution imagery in GE across the Circum-Arctic, we found 445  
260 individual channel networks located in northern Alaska, Russia, and Canada with beaded  
261 morphology (Table 1). This survey was restricted to land areas north of 66° latitude, which was  
262 mainly in the zone of continuous permafrost, though two streams identified were within areas  
263 classified as discontinuous and three within areas classified as sporadic permafrost. The  
264 availability of high resolution snow-free imagery strongly reduced the number identifiable  
265 channels in Siberia and Canada. Extrapolations to the entire region of continuous permafrost  
266 based on the area we could accurately survey, suggests greater than 1900 individual beaded  
267 stream networks with 13% in northern Canada, 18% in Alaska, and 69% in northern Russian  
268 (Table 1). The density of beaded streams in Alaska was estimated to be about 3× higher than in  
269 Russia and 19× higher than Canada, likely related to its small but wide unglaciated, ice-rich  
270 permafrost coastal plain of the Alaska North Slope relative to abundant mountain and foothills  
271 terrain of much of northern Russian and expansive Laurentian Shield covering much of northern  
272 Canada.

273 In Russia, 148 beaded streams were identified and clustered mainly in several different  
274 locations. From East to West these included coastal plains along the Chukchi Sea, lake-rich  
275 valley bottoms west of the Kolyma Delta, mountainous headwaters of the Yakutia Region, higher  
276 elevations of the Yamal Peninsula, and very high densities in the foothills of the Anabar River  
277 Watershed (Fig. 1a). Recent field studies were completed on beaded streams on the Yamal  
278 Peninsula and these researchers also remotely identified channels with beaded morphology in  
279 other Russian taiga and steppe terrains using Google Earth (Tarbeeva and Surkov, 2013).  
280 Comparatively fewer beaded streams were identified across the Canadian Arctic (22 total) (Table  
281 1). This is likely related to regional geology associated with the dominance of exposed bedrock  
282 and thin sediment cover and lack of ice wedges on the Canadian Laurentian Shield. From West  
283 to East, small clusters of beaded streams were found on the coastal plain east of Herschel Island  
284 and south of the Mackenzie River Delta, the lake-rich Tuktoyaktuk Peninsula (Fig. 1c), the  
285 coastal plain around the Coronation Gulf and village of Kugluktuk, and the Banks Peninsula  
286 within Bathurst Inlet, where high resolution imagery was available during this GE survey.

287 Because of greater availability of high resolution imagery, over 60% of the beaded streams  
288 we located were in Alaska even though this was a much smaller area surveyed (Table 1). The

289 southernmost beaded streams in Alaska were found on the coastal plain of the Seward Peninsula  
290 and between Kivalina and Point Hope with an additional cluster higher in the Noatak River valley  
291 (Fig. 2). On the North Slope of Alaska, beaded streams were dense and more evenly distributed in  
292 the western foothills and along the Chukchi coastal plain. Lower densities of beaded streams were  
293 found in the central sand sea region and only a few beaded channels were found on the outer  
294 coastal plain of the Barrow Peninsula and north of Teshekpuk Lake. This lack of channels with  
295 beaded morphology on the outer coastal plain is perhaps unexpected, given the ubiquitous  
296 presence of ice-wedge polygons in which beaded drainage forms. We have observed however  
297 that most channels in this region tend to take a plane bed form without alluvial features, which  
298 may relate to very high pore ice content that in addition to wedge-ice makes soils in this regions  
299 extremely ice-rich, often exceeding 80% by volume (Brown, 1968, Kanevskiy et al., 2013). The  
300 outer coastal plain is also extremely flat with very low drainage densities and very high coverage  
301 of thermokarst lakes and DTLBs (Hinkel et al., 2005), such that all fluvial systems are in low  
302 abundance and the ones present are strongly lake-affected. On the inner coastal plain and  
303 foothills, channels likely develop along moderately sloping terrain with varying densities of ice  
304 wedges, but otherwise low pore-ice content. Thus bead morphology likely develops as ice-wedge  
305 networks thermally erode, yet expansion of pools and runs is confined to the original ice-wedge  
306 casts likely because ice-poor permafrost is more resistant to thermokarst erosion. High densities  
307 of beaded streams were also found throughout the Kuparuk River Watershed from the foothills to  
308 the coastal plain and on the narrower coastal plain east of the Sagavanirtok River to Barter Island  
309 (Fig. 2).

310 Looking at the full set of beaded streams in relation to the ground-ice content of permafrost,  
311 shows that 50% were found on high ground-ice content permafrost, 32% on moderately high  
312 ground-ice content permafrost, and 18% on low ground-ice content permafrost (Fig. 5). Regions  
313 with high ground-ice content were typically associated with either epigenetic permafrost along  
314 the coastal region and syngenetic yedoma permafrost in the foothills region. Approximately 50%  
315 of all beaded streams were found below 60 masl elevation and 90% were found below 210 masl  
316 elevation (Fig. 5). Seven beaded streams were discovered above 500 masl. These were found in  
317 both Alaska and Russia. Our survey did not identify the even higher elevation Imnavait Creek,  
318 861-m elevation (Fig. 2 and 5), since the only high resolution GE imagery for this area was

319 acquired during winter snowcover when beaded morphology could not be observed,  
320 demonstrating the limitations associated with this identification approach. However, such snow-  
321 covered scenes were relatively rare in most imagery we used. Innavaik Creek, along with 12  
322 beaded streams that were identified in our inventory, occur above the Pleistocene Glacial  
323 Maximum (Fig. 2) indicating that streams with beaded morphology can readily form in glaciated  
324 terrain.

325 In our aerial surveys across the Alaskan North Slope, we located 43 beaded streams from  
326 three transects covering 436 km of flight lines or approximately 220 km<sup>2</sup>, suggesting a density of  
327 0.20 streams per km<sup>2</sup> or a drainage density of roughly 0.10 km/km<sup>2</sup>. Comparing transect lines to  
328 landscape classification of permafrost ground-ice content shows that these surveys covered 29%  
329 low, 59% moderate, and 12% high categories (Fig. 2). However, of the recognized beaded  
330 streams along these courses, a much higher proportion was associated with moderate ice-rich  
331 permafrost (76%). Only three streams occurred on high ground-ice content permafrost, two on  
332 very flat outer coastal plain areas with glaciomarine sediments, and one in yedoma deposits of the  
333 foothills (Fig. 2). The majority of stream channels on the outer coastal plain, with very low  
334 drainage densities, would be generally classified as plane bed (Montgomery and Buffington,  
335 1997) or F5-6 from Rosgen's Classification (Rosgen, 1994), and also have been termed lacustrine  
336 channels (Arp et al., 2012b) because they are nearly all fed mostly by lakes. Still, polygonized  
337 tundra tends to be more pronounced and uniform in this region, and so a general lack of channels  
338 with beaded morphology was unexpected.

339 Beaded streams in the Fish Creek Watershed range from 6 to 125 m elevation and the full  
340 range of permafrost, ground-ice contents (Jorgenson et al., 2008). We inventoried 126 beaded  
341 streams as individual catchments or drainage networks within this 4700 km<sup>2</sup> watershed located on  
342 the inner Arctic Coastal Plain of northern Alaska (Fig. 3). Based on previous analysis of lakes,  
343 streams, and river channels here (Arp et al., 2012b), beaded streams represent 1168 km of  
344 channel length or 47% of the entire fluvial system. The equivalent drainage density of beaded  
345 stream channels is 0.25 km/km<sup>2</sup>. Estimated drainage densities for the broader regions surveyed  
346 with GE were far lower compared to this watershed (Table 1).

347 Since the majority of beaded streams on the ACP initiate as 1<sup>st</sup>-order channels below  
348 thermokarst lakes or DTLBs (Arp et al., 2012b), their distribution throughout the Fish Creek  
349 Watershed is linked to lake distribution (Fig. 3). The exception to this pattern is in the headwaters  
350 of Judy Creek that form a narrow arm extending into eolian silt deposits with bedrock outcrops.  
351 In this area, lake densities are low and many streams initiate as colluvial channels (Arp et al.,  
352 2012b), which then transition to beaded morphology downstream, similar to patterns reported for  
353 the higher elevation foothills of the Kuparuk watershed (McNamara et al., 1999). An example of  
354 this drainage pattern is also evident in Fig. 1a. Thirteen percent of all beaded streams in the Fish  
355 Creek Watershed are located within this region of ice-rich eolian loess. Relatively lower densities  
356 of beaded streams occur in the eolian sand sea regions (western half of Fish Creek Watershed)  
357 where permafrost is classified as having low ground-ice content (Fig. 2) and where most lakes  
358 formed between relict dunes (Jorgenson and Shur, 2007) and are up to 20 m deep (Arp et al.,  
359 2012b). The highest densities of beaded streams occur in the lower Fish Creek Watershed where  
360 surface geology is dominated by alluvial and marine silts and sands with some pebbly deposits  
361 and permafrost is moderately ice-rich (Carter and Galloway, 2005). Our results suggest some  
362 variation in beaded stream distribution within the inner coastal plain, particularly with lower  
363 densities associated with eolian and alluvial sand deposits and higher densities on marine and  
364 loess silt deposits. However, we still find that beaded streams are often the dominant form of low-  
365 order channels throughout a wide range of permafrost terrain on the Alaska North Slope and this  
366 is likely the case in much of northern Russia as well (Tarbeeva and Surkov, 2013).

367

### 368 **3.2 Morphology in relation to landscape and watershed positions**

369 Since abundant large, deep pools are the defining characteristic of streams with beaded  
370 morphology, we initially classified and quantified these channels according to pool (bead)  
371 morphology and density (Fig. 6). On a reach scale (100's of meters) or segment scale (up to  
372 several km between tributary junctions), pool density, form, and size was often distinct.  
373 However, on a more extensive drainage network scale, which is the scale we used for  
374 classification, pool density varied to a greater extent. Counts of pools from high resolution CIR  
375 photography showed densities ranging from 2 pools per 100 m of channel up to 10 per 100 m

376 (Fig. 6). Lachenbruch (1966) suggested that polygon spacings range from 5-m to 50-m based on  
377 variation in ground strength and the width of stress relief zones, which approximately matches the  
378 range of beaded densities reported here. This indicates that local controls, such as size, pattern,  
379 and form (i.e., low- and high-centered polygons) of tundra or broader-scale thermokarst  
380 landforms such as DTLBs (Frohn et al., 2005; Hinkel et al., 2005), may be the main cause of such  
381 variability in channel morphology.

382 Of the 126 individual beaded channel networks in the Fish Creek Watershed, 40% were  
383 classified as elliptical with distinct connecting runs, 17% had mostly coalesced pools and short or  
384 non-existent runs, 34% predominantly had irregularly shaped pools, and the remaining 8% were  
385 classified as connected thaw pits (Figs. 4 and 6). The majority of beaded channels are shown to  
386 initiate from either lakes and DTLBs (Arp et al., 2012b) and these took a wide range of pool  
387 forms downstream. In the Fish Creek Watershed, most channels with small elliptical pools were  
388 located in the higher elevation areas associated with eolian sand and loess deposits compared to  
389 lower elevation marine sand and silt deposits. Whether this pattern relates to size and form of ice-  
390 wedge networks that develop in sandy soils or how eroding sandy soils moderate expansion by  
391 infilling pools or interactions with vegetation deserves further consideration. The other channel  
392 classes were more evenly distributed throughout the watershed and by surficial geology.

393 Comparing channels of entire watershed by individual slope and drainage area helps  
394 understand how the larger drainage network is organized from channel initiation points (channel  
395 heads) to larger alluvial sand-bedded channels (Fig. 7). This slope-area relationship is consistent  
396 with patterns more universally observed across a wide range of drainage networks (Montgomery  
397 and Buffington, 1997; Montgomery and Dietrich, 1989; Whiting and Bradley, 1993). In the Fish  
398 Creek Watershed, channels initiating from hillslopes are steepest with slopes averaging 2% and  
399 with drainage areas  $<1 \text{ km}^2$ . Channels initiating from lakes, which all form beaded streams, had  
400 average slopes of 0.4 % and drainage areas  $> 1 \text{ km}^2$  (Fig. 7). Channel initiation thresholds  
401 reported for the foothills beaded stream Imnavait Creek are  $0.02 \text{ km}^2$  (McNamara et al. 1999)—  
402 roughly one and two orders of magnitude smaller than hillslope and lake initiated channels,  
403 respectively, in this ACP watershed. Because beaded channels compose approximately half of the  
404 drainage network in the Fish Creek Watershed (Arp et al., 2012b), they correspondingly have a  
405 wide range of drainage areas ( $2 - 54 \text{ km}^2$ ) and slopes ( $<0.1 - 0.8\%$ ) (Fig 7). Analysis of beaded

406 channels in Yakutia, Russia show a narrower range of drainage areas (3 – 10 km<sup>2</sup>) with slopes  
407 less than 0.2 % (Tarbeeva and Surkov, 2013). Alluvial channels form the higher order portions of  
408 most drainage networks and in the Fish Creek Watershed typically begin at drainage areas > 40  
409 km<sup>2</sup> and channel slopes less 0.03% (Fig. 7).

410 To better understand how beaded streams fit within fluvial systems of the ACP and evaluate  
411 what controls their morphology, we selected two drainage networks for more detailed analysis of  
412 longitudinal channel dynamics from headwaters downstream (Fig. 8). Fish Creek has its  
413 headwaters near the western divide of the watershed at 78 masl. It is located entirely within the  
414 eolian sandsheet and initiates from a deep depression lake (Fig. 3). This channel network first  
415 flows through several more depression lakes and in between maintains a classic beaded  
416 morphology (Fig. 4a). Over the next several km, the channel cuts through both vegetated and  
417 unvegetated sand dunes, which likely supply coarse sediment. The channel also contacts steeper  
418 hillslopes that could contribute sediment as well. This portion of the channel appears transitional  
419 since reaches of beaded morphology are interspersed with more sinuous channels having point  
420 bars and meander cut-banks (Fig. 8a). At km 20 downstream, the channel steepens considerably  
421 below a tributary fed by a DTLB and then cuts through two more sand dunes, before taking a  
422 more even slope for the remaining 110 km with sand-bedded alluvial characteristics. Thus, Fish  
423 Creek quickly transitions from beaded to alluvial morphology likely because of ample sediment  
424 supply associated with the eolian sand landscape (Fig. 6A).

425 The other system we analyzed, the Ublutuoch River (Fig. 3), begins at a lower elevation than  
426 Fish Creek, 58 masl, in the southern portion of the watershed at the eastern margin of the eolian  
427 sandsheet. The channel initiates from a large set of coalesced depression lakes, totaling about 5  
428 km<sup>2</sup>, seen as the flat profile in Fig. 8b. The first 12 km of this stream are relatively steep with  
429 regular density of pools typical of beaded morphology. Several oxbow lakes occur lower in this  
430 segment, indicative of channel migration, but the Ublutuoch then flows through several more  
431 lakes, likely trapping all sediment and resetting the system to a beaded form with a flatter slope.  
432 At km 24 downstream, a tributary from a large DTLB enters from the north, and at this point the  
433 channel starts taking a more sinuous form with oxbow lakes and other floodplain features (Fig.  
434 8b). We suggest that this segment of stream from 24 to 56 km is transitional between beaded and  
435 alluvial morphology—a much longer transition than was observed along upper Fish Creek.



436 Surrounding uplands here are entirely within the zone of marine silt and sand without distinct  
437 sediment contributions from adjacent sand dunes. Near the end of the segment, the channel  
438 becomes much more sinuous with oxbows and meander scars becoming evident, yet regular pools  
439 (beads) persist. At km 56, the stream contacts a distinctly higher hillslope that we think supplies  
440 sediment to the channel and after which it takes on a distinct alluvial form lacking any evenly  
441 spaced beaded morphology (Fig. 8b). During the entire transitional channel course, the slope is  
442 nearly constant at about 0.02 – 0.04%. It then flattens greatly to <0.01% over the last 5 km and  
443 becomes quite deep (exceeding 5 m in some pools) and very sinuous (2.3) with high, regular  
444 banks before its confluence with Fish Creek.

445

### 446 **3.3 Channel change and formation**

447 To evaluate the hypothesis that beaded streams form in ice-wedge networks and that pools  
448 progressively expand over time, more detailed studies were conducted in one system, Crea Creek,  
449 in the lower Fish Creek Watershed (Fig. 3), to look at decadal scale changes and estimate its time  
450 of formation. Using remote sensing change detection over 64 years, we found no changes in the  
451 channel position along this 2.7 km segment (Fig. 9). The total number of pools in this segment  
452 remained relatively stable, though tracking individual beads showed that 18% disappeared or  
453 could not be observed from 1948 to 2013 and a similar number of new pools (19%) were  
454 identified in 2013 that could not be observed in the 1948 imagery (Table 2). The majority of these  
455 were very small (diameters <4 m) and we think it is likely that changes in vegetation or variation  
456 in water levels between images may have obscured their detection. The mean pool size in 1948  
457 was 60 m<sup>2</sup> compared to 62 m<sup>2</sup> in 2013, resulting in little net change in total pool area over this  
458 period. Tracking the size of individual pools found in both images showed that about one-third  
459 shrank by more than 10% surface area, about one-third expanded by more than 20% surface area,  
460 and the remaining pools were essentially unchanged. Thus, our analysis suggests progressive  
461 expansion of these thermokarst landforms, yet the channel course appeared entirely unchanged  
462 over this period. For comparison to other thermokarst landforms, thermokarst lakes in this region  
463 also progressively expand their lake basins, 0.10 m/yr on average (Jorgenson and Shur 2007), but  
464 can drain catastrophically if a shoreline expands beyond a lower gradient or is breached by

465 another lake or migrating river (Grosse et al. 2013). Alluvial channels on the ACP are considered  
466 highly dynamic often with very high rates of bank erosion due to interactions with permafrost  
467 such that major changes in channel course can occur over short time periods (Scott 1978). Our  
468 observations of a stable course along Crea Creek over 64 years, along with an apparent lack of  
469 beaded channels that appear abandoned on the ACP, suggest long-term behavior more similar to  
470 bedrock channels (Wohl 2000). Tarbeeva and Surkov (2013) rather suggest the beaded streams  
471 are transient features and become easily filled with sediment from headwater thermokarst and  
472 other hillslope erosive processes. We suggest that sediment delivery plays a role in how beaded  
473 streams transition to other fluvial forms, but this typically operates at lower positions in the  
474 watershed.

475 We also delineated the riparian zone or gulch of this beaded stream, indicated in plan-view  
476 by higher moisture and the contrast between upland tussock tundra and vegetation composed of  
477 willows, tall sedges, and dwarf birch, to see if other changes beyond the main channels were  
478 evident. (Table 2). Such changes could correspond to progressive subsidence of ice-rich  
479 permafrost by thermokarst degradation or shrub expansion as has been noted throughout many  
480 areas of the Arctic (Sturm et al., 2001). Consistent with what can be observed in the shorter  
481 reaches in Fig. 9, the overall change in riparian gulch width was slight, a 9% increase (Table 2).  
482 Analysis of repeat photography in this same area has shown a recent increase in degrading ice-  
483 wedge polygons to form thaw pits (Jorgenson et al., 2006). We also recorded and tracked thaw  
484 pits (ice-wedge junctions with ponded water) between the two images within a 100-m zone on  
485 either side of the channel, but outside of the riparian gulch. This showed a somewhat similar  
486 pattern as was found when tracking pools in the channel of Crea Creek. In total, we found 120  
487 individual thaw pits or 1 pit per 2500 m<sup>2</sup>, typically in clusters associated with high centered  
488 polygons. In 1948 we found 74 thaw pits, 55 of which were not observed in 2013, and in 2013 we  
489 found 66 thaw pits, 47 of which were not observed in 1948 (Table 2). This suggests that thaw  
490 pits may progress through a form of succession in which they degrade, collect water, paludify  
491 and/or partly drain or dry, such that detection is obscured after several decades. This is a similar  
492 sequence as demonstrated for denser networks of thaw pits in polygonized tundra in adjacent  
493 upland areas of the Fish Creek Watershed (Jorgenson et al., 2006). We suggest that beaded  
494 channels may evolve in a similar manner with most pools gradually expanding and some

495 contracting with changing vegetation. Such behavior seems particularly apparent in viewing  
496 coalesced beads of some channels (Fig. 4c). Yet our impression based on this photographic  
497 comparison and qualitative observation of other channels with repeat photography is that channel  
498 courses and networks appear to behave more like bedrock channels that are set in place and  
499 potentially very old.

500 Analyzing the stratigraphy and geochronology of sediments in a large pool of Crea Creek  
501 may attest to the timing of stream channel formation and the depositional environment since  
502 initiation. A fibrous organic-rich layer with abundant terrestrial plant material separated the  
503 transition from organic-poor medium-grained sand to organic-rich silty sediment that is the  
504 uppermost unit—we interpreted this layer as basal sediments that were dated to 9.0 ( $\pm 40$ ), and  
505 13.6 ( $\pm 215$ ) ka cal years BP (Fig. 10). The terrestrial macrofossils (shrub twigs) in this fibrous  
506 unit and the two dates that span 4 ka suggest this layer may have been a terrestrial soil that  
507 persisted for millennia on top of eolian or alluvial sand deposits, but predated the initiation of the  
508 beaded stream pool. Alternatively, this layer may represent the depositional environment of an  
509 early stage of the beaded stream pool where terrestrial vegetation was overhanging and being  
510 deposited, and adjacent soils were being eroded by ice wedge degradation and supplying a range  
511 of reworked material with different  $^{14}\text{C}$  ages to be deposited onto this fibrous layer. Regardless,  
512 we interpret the 9.0 ka moss macrofossil sampled from the upper portion of the fibrous layer to be  
513 a conservative upper limit age on the initiation of the beaded stream pool. At this time, we do not  
514 know whether the lower limit of this age estimate is near the 9.0 ka time period, or represents the  
515 late Holocene. The large age-gap from 9.0 ka at 42 cm to  $\sim 0.7$  ka at 22 cm suggests that either a  
516 water-level lowering event caused a hiatus of sedimentation through much of the Holocene, or  
517 that high flow events or other processes eroded the sediment deposits representing most of the  
518 Holocene (Fig. 10). However, there was no preserved wetland or terrestrial soil layer interrupting  
519 the *gyttja* unit, which would have accompanied a water-lowering event. The Crea beaded stream  
520 pool we examined appears to have had episodic sedimentation during the Holocene that is  
521 periodically eroded by either high flow events, or ice scouring.

522 The stratigraphy and  $^{14}\text{C}$  dates from a core in a deep pool in Blackfish Creek also suggest  
523 unconformities in sedimentation of beaded stream pools. The Blackfish pool had sandy organic-  
524 rich *gyttja* with several 3-6 cm bands of coarse sand that graded upward to fine sand. These

525 suggested upstream scouring events that mobilized and transported high and coarse sediment  
526 loads episodically, potentially from the catastrophic drainage of upstream lakes. A number of  
527 DTLBs occur upstream of this site and their drainage dates are currently unknown, but may  
528 correspond to these events. The basal age of this unit from a sedge fragment yielded a date of 590  
529 ( $\pm 30$ ) yrs BP, considerably younger than we found at Crea Creek (Fig. 10). A paired sedge and  
530 willow macro-fossils extracted from above a coarse sand horizon at 20-30 cm indicated ages of  
531 1430 ( $\pm 25$ ) years BP and 125 ( $\pm 25$ ) years BP. Our interpretation of this core and analyzed ages is  
532 that the basal material was either not reached or had been remobilized and that a number of very  
533 high flow events in this stream's recent history had deposited material from upstream of varying  
534 ages. These flow events may have partially eroded some of the late-Holocene record and / or  
535 deposited reworked macrofossils, which yielded less certain  $^{14}\text{C}$  ages. The depositional  
536 environments of beaded streams seem discontinuous and difficult to interpret because of  
537 unconformities and reworked plant macrofossils. In the right situation however, pool sediments  
538 may record upstream watershed events such as lake drainage, as we think is preserved in the  
539 Blackfish Creek core. At this time, the typical lifespan of the beaded streams we studied remains  
540 uncertain, but our best estimate places the Crea Creek channel's formation near the Pleistocene-  
541 Holocene transition. The Blackfish Creek core was much more complicated and provided no  
542 apparent clues to the age of this beaded channel.

543

## 544 **3.4 Physical processes affecting morphology and habitat**

### 545 **3.4.1 Winter Processes**

546 Because winter is the dominant season in the Arctic and most beaded streams are ice-covered and  
547 likely stop flowing from October to late May or early June, understanding their state during this  
548 period is of great interest. An important characteristic of beaded stream channels on the ACP is  
549 that their often deep gulches, 0.5 – 2.0 m, rapidly fill with blowing snow early in the winter,  
550 effectively leveling the snow-surface topography with the surrounding tundra. This deep snow  
551 insulates ice on pool surfaces, reducing its rate of thickening, and impacting soil active-layer  
552 dynamics as well. Measured snow depths above beaded streams averaged 122 cm and ranged  
553 from 70 cm on a small pool in Crea Creek to 192 cm above a pool in Bill's Creek (both in the

554 lower Fish Creek Watershed) (Fig. 11). In contrast, surrounding tundra snowpack rarely exceeds  
555 40 cm depth by late winter. Not only does this thick snowpack insulate ice and soil, but it also  
556 persists much longer in the spring and contributes a much larger portion of snow-water per unit  
557 area directly to runoff (Arp et al., 2010). For 12 beads we surveyed from 2010 to 2013, only one  
558 was found to be entirely frozen to the bed by March or April (Fig. 11). A more detailed and  
559 extensive survey of water below ice were conducted in March and April of 2013 using ground-  
560 penetrating radar (GPR) and high resolution synthetic aperture radar (TerraSAR-X) in this area  
561 and found the majority of pools had liquid water below ice (Jones et al., 2013). Average ice  
562 thickness of pools surveyed was 106 cm and ranged from 89 cm to 129 cm (Fig. 9). For  
563 comparison, lake ice thickness in this same region and years ranged from 118 cm in 2011 to 171  
564 cm in 2013 (Arp et al., 2012a; Jones et al., 2013). The average depth of water we found below the  
565 ice was 44 cm and ranged from 4 cm up to 106 cm (Fig. 11). This water was typically under  
566 pressure from ice expansion and the weight of snow, such that upon drilling through the ice,  
567 water typically floods the frozen pool surface. On at least two occasions live fish (Alaska  
568 blackfish, *Dallia pectoralis*) were pushed out of the drill hole to the surface by flowing water  
569 during these surveys. Monitored dissolved oxygen levels in one bead showed a rapid drop to  
570 hypoxic conditions by mid-January and measurements in March typically showed levels below  
571 5% of saturation or <1 mg/L. Alaska blackfish, however, are known to tolerate such conditions  
572 (Scott and Crossman, 1973; Crawford, 1974), providing evidence that some beaded stream pools  
573 can function as overwintering habitat for select Arctic fish species. While we suspect that these  
574 stream pools are not preferred overwintering locations for most fishes, these relatively warm  
575 unfrozen sediments may be important habitat for invertebrate and microbial communities.

576 Despite the relatively small diameter of pools, thawed sediment underlie most of them and  
577 measured depths averaged 120 cm and were up to 170 cm in one pool with sand-gravel sediment  
578 (Fig. 11). Similar talik depths are reported for pools or broadenings in beaded channels in Russia  
579 (Tarbeeva and Surkov, 2013). This suggests that beaded stream channels further disrupt the  
580 ground thermal regimes of otherwise continuous permafrost landscapes at a scale relative to their  
581 size, whereas large river channels and lakes with floating ice result in taliks reaching 10's of m  
582 deep or more (Brewer, 1958; Lachenbruch et al., 1962). Since 2009, we have been monitoring  
583 bed temperatures in a set of pools within beaded stream systems in the lower Fish Creek

584 Watershed. Typically winter bed temperatures rapidly approach the zero-degree curtain and  
585 average winter temperatures (November to April) consistently average 0°C ( $\pm 0.1$ ). Similarly,  
586 mean annual bed temperatures (MABTs) fall within a narrow range averaging 2.9°C and varying  
587 interannually almost entirely according to summer temperatures (Fig. 12a). Such MABTs above  
588 freezing, also suggest the presence of a talik (Burn, 2002; Ensom et al., 2012), as we confirmed  
589 with field measurements. The presence of year-round unfrozen sediment and some liquid water in  
590 pools may be an essential factor supporting microbial- and invertebrate-based food webs, which  
591 then feed summer productivity and the use of beaded streams as important foraging habitat.  
592 Additionally, perennially thawed sediment also likely enhances the survival and productivity of  
593 macrophytes that provide additional habitat and forage.

594

### 595 **3.4.2 Summer Processes**

596 Much of the variation in MABT of pools is determined by whether pools become thermally  
597 stratified during the summer. Monitoring of surface temperatures relative to the pool beds and  
598 temperature in the channel runs suggests a wide range of mixing behaviors and stratification  
599 regimes among pools both between different stream systems and from pool to pool in a single  
600 stream. For example in three beaded streams monitored from 2009-2012, a 1.3-m pool never  
601 became stratified, another 1.4-m pool was stratified by 10% or more (i.e., surface temperature /  
602 bed temperature > 1.1) for 13 days per summer on average, and a 2.1-m pool had a stratification  
603 ratio of 1.2 and was stratified for over a month on average per year (Fig. 12b). This generally  
604 suggests that deeper pools stratify to a greater degree and for longer periods. To assess interpool  
605 variability, we instrumented an additional three pools in Crea and Blackfish creeks from June  
606 2013 through August 2013 with surface and bed thermistors. In Crea Creek with pools depths of  
607 1.6, 1.7, and 2.0 m, corresponding average stratification ratios (and durations with ratios >1.1)  
608 were 1.05 (5 days duration), 1.09 (23 days), and 1.03 (4 days), respectively (Fig. 12b). In  
609 Blackfish Creek with deeper and coalesced pools, instrumented pools were 1.5, 2.2, and 2.6 m  
610 depth and corresponding stratification ratios and durations were 1.04 (5 days), 1.16 (24 days), and  
611 1.10 (19 days). Thus, there is as expected some relationship between pool depth and stratification,  
612 but this is generally weak and suggests other factors control how water mixes among different

613 pools. A single densely instrumented pool in Imnavait Creek was shown to stratify in a complex  
614 and dynamic manner (Merck and Neilson, 2012), similar to more extensive work completed there  
615 originally (Oswood et al., 1989). The velocity of upstream runs and morphology of pools at run  
616 inflows is certainly one factor. A steeper run upstream of Bill's Creek was likely the cause of  
617 continuous mixing during all flows, ambient air temperatures, and wind regimes, which produced  
618 higher MABTs (Fig. 12a) and possibly the deepest talik we measured (Fig. 11).

619 The extent and structure of emergent aquatic macrophytes in pools likely also plays a role,  
620 where some shallow beads have very dense macrophytes beds (*Potamogeton* spp., *Arctophila*  
621 *fulva*, and *Hippuris vulgaris* are the most common plants) that likely create a rough and thick  
622 boundary layer enhancing stratification. Adjacent pools of seemingly similar depth and surface  
623 area are often devoid of vegetation, creating greater habitat heterogeneity within beaded stream  
624 systems. Variation in water color due to dissolved organic carbon may play some role, however  
625 rarely do beaded streams in this part of the ACP have highly stained water from organic acids as  
626 has been observed in other beaded stream systems at foothills locations (Merck and Neilson,  
627 2012; Oswood et al., 1989).

628 Ecologically, the important point in terms of fish habitat is that within a single beaded  
629 stream, varying degrees of mixing and thermal stratification from pool to pool likely create a  
630 range of temperature zones that can be utilized to either avoid thermal stress or optimize  
631 energetics for foraging and other activities. For example, some salmonids behaviorally  
632 thermoregulate by moving to warmer areas after foraging bouts in cooler water in order to  
633 accelerate metabolism and assimilate more quickly (Armstrong et al., 2013). Stratification within  
634 a single bead and heterogeneity in thermal characteristics of nearby beads within a network may  
635 provide similar opportunities to behaviorally optimize growth and foraging efficiency during  
636 summer. This thermal variability may also play a key role in the distribution of fish prey items,  
637 including the forage fish ninespine stickleback (*Pungitius pungitius*) as well as invertebrate and  
638 plankton communities (McFarland, 2012).

639 Similar to the development of stratification in Arctic lakes, stream pools tend to stratify  
640 starting in early July following snowmelt runoff and associated cold temperatures and turbulent  
641 mixing. An episode of intense summer warming leading to stratification was clearly observed in

642 pools at Crea and Blackfish creeks starting on 9-July 2013 when the surface water temperature  
643 rose rapidly from 8 to 16°C over several days while beds warmed more slowly, albeit to differing  
644 degrees (Fig. 13). In Crea Creek, the mean daily temperature difference between the pool surface  
645 and bed was as high as 2.5°C in one pool and only 0.9°C in the other (Fig. 13a). For the same  
646 warming event in Blackfish Creek, levels of stratification were 1.1°C in one pool and 4.7°C in the  
647 other (Fig. 13b). Another warming event in late July caused even higher stratification, up to 5°C,  
648 in pools of both streams.

649 In beaded streams on the ACP, we have observed that peak flows predictably occur only one  
650 to two days after streams begin to flow initially, which is first on top of the ice and often partly  
651 beneath the rapidly melting snowpack in stream gulches. Over five years of gauging on five  
652 separate beaded streams, the timing of peakflows ranged from 1-Jun to 10-Jun with peak hourly  
653 discharges of 1 – 10 m<sup>3</sup>/s, which typically exceeds summer flows by two orders of magnitude or  
654 more. This fast consistent response is similar with that observed for larger river systems of the  
655 ACP (Arp et al., 2012b; Bowling et al., 2003), which are fed predominantly by beaded streams  
656 and their source-water lakes. A related characteristic is that water temperatures are very near 0°C  
657 at flow initiation and rise very rapidly directly following peak discharge, often warming to 10°C  
658 or more over a 2-3 day period (Fig. 13). These rapid changes in flow and temperature regimes  
659 may provide important cues to fish migrating along larger river courses fed by beaded streams.  
660 Arctic grayling (*Thymallus arcticus*) are known to seek habitats that warm most rapidly in the  
661 spring to spawn, and the quickly rising temperatures of beaded streams may contribute to their  
662 importance as spawning habitats (Heim, 2014). In fact, we often see individual fish migrating up  
663 beaded channels with water flowing over bedfast ice just prior to peakflows, when their dark  
664 bodies can be easily observed crossing the white ice surface. Tracking studies of Arctic grayling  
665 tagged in Crea Creek, show a rapid pulse of upstream migration into the system during and after  
666 peakflow (Heim, 2014). This early upstream migration may represent an adaptation to maximize  
667 time spent in productive spawning habitats at the earliest possible time in order to provide a  
668 longer period of growth for offspring.

669 More broadly, the period of peak flow across this hydrologic landscape represents a period of  
670 high connectivity among aquatic habitats, where fish can disperse from relatively limited  
671 deepwater overwintering habitats and move into shallow, seasonally-flowing habitats like beaded



672 streams. Again in late August through September, changes in flow and temperature may become  
673 important environmental cues that fish use to time migratory movements out of beaded streams  
674 (Heim, 2014). Migration out of Crea Creek in the fall was strongly correlated to decreases in  
675 stream temperature, as the channel connection to the Ublutuoch River became restricted due to  
676 ice formation. Low flows and colder temperatures increase the risks of utilizing Crea Creek  
677 (Arctic grayling were not found to overwinter within the drainage), yet persistence of fish within  
678 the drainage through September may be advantageous in terms of growth and acquisition of  
679 energy reserves prior to the onset of winter (Heim, 2014).

680 With respect to the basic physics of flow through stream systems characterized by multiple  
681 evenly spaced pools (storage zones), the attenuation of flows seems intuitive. This has  
682 implications for streamflow dynamics, movement and transformations of solutes (carbon,  
683 nutrients, and contaminants), the transport of particles including mineral and organic sediment,  
684 plankton (both semi-mobile and drift), and the movement of fish. Because most beaded streams  
685 are set within a permafrost framework without interactions with groundwater systems, the  
686 development of hyporheic flow through bed material or banks is unlikely. Storage processes  
687 have been investigated in Imnavait Creek and adjacent beaded streams around Toolik Lake in  
688 Alaska where the glaciated setting and corresponding porous substrates, and known spring  
689 systems, may allow hyporheic storage to play a significant role in beaded stream hydrology  
690 (Merck et al., 2012; Zarnetske et al., 2007). Still we suggest that the characteristic large size and  
691 frequency of pools of beaded streams strongly dominates transient storage, even when  
692 groundwater systems are present allowing hyporheic exchange, which is probably rare in  
693 continuous permafrost zones of the ACP where surface-water interactions with ground-water are  
694 absent.

695 The distribution of water velocity at the reach-scale in a beaded stream with large, deep and  
696 coalesced pools (Blackfish Creek) compared to a stream with shallower elliptical pools (Crea  
697 Creek) using tracer tests highlights how such morphology functions in water storage and  
698 residence time (Fig. 14). For example, the much more rapid velocities observed in an alluvial  
699 channels with otherwise similar discharge and slope underscores this impact on dense, evenly  
700 spaced pools have on the hydrologic functioning of beaded channels. A similar range of reach-

701 scale velocities are reported when comparing beaded channels to other channel types in Arctic  
702 drainage networks (Tarbeev and Surkov, 2013, Zarnetske et al., 2007).

703 Residence times of water in these two beaded channels increase predictably with  
704 decreasing flows and relatively higher storage areas (Table 3). At the start of peakflow recession  
705 over 10% of the water in both channels was still moving at velocities lower than 0.1 m/s. During  
706 summer flows, the fastest reach-scale velocities did not exceed 0.2 m/s in Crea Creak and 0.05  
707 m/s in Blackfish Creek. Even though individual run velocities often exceed 0.5 m/s or greater,  
708 the water in the channel exchanges with storage zones (pools) sufficiently to slow the total  
709 movement of water by up to an order of magnitude or much more. Such slow transport rates of  
710 water in beaded stream systems may have important implications for maintaining in-stream flow  
711 during dry summers when evapotranspiration far exceeds rainfall on daily to weekly time-scales.  
712 The major source of water to these channels are upstream lakes (Arp et al., 2012b; Bowling et al.,  
713 2003), and the evenly spaced storage-rich nature of these streams may function to maintain more  
714 constant flows and reduce evaporative losses during summer drought periods.

715 The summer of 2013 when these experiments were conducted was very wet and rainy  
716 compared to previous years when we have monitored discharge in these streams. Still, in five  
717 years of monitoring, starting in the summer of 2008, we have not yet observed interruptions in  
718 flow during summer drought periods in five gauged streams. At least some alluvial streams in  
719 the Arctic foothills of Alaska have experienced prolonged periods of no flow over certain reaches  
720 during drought conditions when only minimal flow through interstitial gravels disrupt migration  
721 of Arctic grayling (Betts and Kane, 2011). In some instances, individual Arctic grayling have  
722 been observed traveling over 160 km within a year visiting different key habitats within a  
723 “migratory circuit” (West et al., 1992). Thus, connectivity among spatially separated habitats is  
724 critical to this life history strategy, and beaded streams may function in maintaining hydrologic  
725 connectivity and fish passage between alluvial rivers and tundra lakes and ponds. Extreme  
726 drought conditions occurred on the ACP and foothills during the summer of 2007 and the  
727 hydrologic response has been well documented in rivers (Betts and Kane, 2011; Arp et al.,  
728 2012b), thermokarst lakes (Jones et al., 2009a), and upland tundra (Jones et al., 2009b) in this  
729 region. Whether beaded streams in this area maintained hydrologic connectivity between river

730 and lake systems through this dry summer was undocumented and warrants reconstruction  
731 through hindcast modeling.

732 The other key function that the hydraulics of beaded streams provides is productive foraging  
733 habitat for Arctic fishes. This stems from the observation that larger foraging fishes (e.g., Arctic  
734 grayling) spend much of their time holding in channel runs downstream of pools, where they  
735 efficiently ambush drifting zooplankton, invertebrates, and nine-spine stickleback (McFarland,  
736 2012). The rapid shift in velocities from pools to runs may function as a key delivery system of  
737 forage that either resides primarily in beaded stream pools (i.e., ninespine stickleback and aquatic  
738 macroinvertebrates) or comes downstream as drift from lakes (i.e. zooplankton) or laterally from  
739 riparian vegetation (i.e. terrestrial invertebrates). Such a setting may in part be the same reason  
740 why lake inlets and outlets are such productive ecosystems (Jones, 2010). The difference here is  
741 that along the course of beaded streams, this lake outlet delivery system is replicated multiple  
742 times over a short distance (i.e., 5 times per 100 m on average, Fig. 6). Approximately half of the  
743 Fish Creek drainage network is composed of beaded streams, the equivalent of 1200 km of  
744 stream length (Arp et al., 2012b). If we assume a pool density of 5 per 100 m, this gives us an  
745 estimated 60,000 pools (beads) throughout this watershed. Recently, the development of a Fish  
746 Creek Watershed classification of lakes >1 ha shows 4,362 lakes, of which 45% have perennial  
747 stream outlets and another 30% have at least ephemeral outlets (B.M. Jones, unpublished data). In  
748 terms of potential fish habitat for summer foraging, this comparison suggest that pools in beaded  
749 streams increase the number of potential fish habitat zones for ambush foraging by 18-fold across  
750 the landscape over lake inlets and outlets alone.

751

## 752 **4 Conclusions**

753 This body of research on beaded streams in continuous permafrost landscapes documents a wide  
754 and varied distribution across the Circum-Arctic in relation to ground-ice content in the upper  
755 permafrost, topography, and elevation. On the inner coastal plain of northern Alaska, our surveys  
756 indicate that beaded streams compose the majority of drainage networks and most channels  
757 initiate from and are fed by lakes. At least in northern Alaska, lakes supply water for new  
758 development in the form of ice roads and other industrial and municipal uses. Knowing how such

759 practices affect downstream ecosystems warrants investigation. Channels with beaded  
760 morphology are maintained downstream, eventually forming alluvial channels in relation to  
761 varied water and sediment supply. This suggests that new land disturbances, such as road  
762 construction or thermokarst processes that can alter these watershed fluxes, will factor into future  
763 drainage network changes. It also appears that beaded stream channels are relatively stable over  
764 time and potentially very old, such that any observations of rapid channel change may be  
765 indicative of more extreme forcing agents, either anthropogenic or climate driven. Given these  
766 concerns and the high density of beaded stream systems in many Arctic landscapes, expanded  
767 research into the role of these ecosystems in permafrost, hydrological, and biological processes  
768 will be essential.

769 The coupled biophysical processes of beaded stream systems that provide key ecosystem  
770 functionality are described conceptually in Fig. 15. We found high spatial and temporal thermal  
771 variability among pools, which likely play an important role in permafrost thaw and coldwater  
772 habitat (Fig. 15a). Beaded morphology appears to also play an important role in summer feeding  
773 habitats and hydrologic connectivity for migrating fish, the quality and availability of which is  
774 critical during short Arctic summers. During long Arctic winters, beaded stream gulches fill with  
775 deep snow that effectively insulates ice and permafrost and plays a role in creating taliks and  
776 providing overwintering habitats for certain fish and invertebrate communities (Fig. 15b). This  
777 conceptual understanding of beaded stream systems helps summarize seasonal and reach-scale  
778 ecosystem functions of interest to physical and biological scientists including managers  
779 concerned with changing human uses of Arctic lands and waters.

780

781

## 782 **Acknowledgements**

783 This research was supported primarily by the Bureau of Land Management's Arctic Field Office  
784 and the Arctic Landscape Conservation Cooperative. Additionally funding was provided by  
785 Alaska EPSCoR Northern Test Case (OIA-1208927), Circumarctic Lake Observation Network  
786 (ARC-1107481), and the National Fish and Wildlife Foundation. We thank F. Urban, R.

787 Kemnitz, C. Couvillion, M. Lilly, J. Adams, J. Derry, H. Toniolo, J. Webster, and J. McFarland  
788 along with numerous helicopter pilots and ConocoPhillips-Alaska, Inc. (Alpine Facility) for  
789 assistance with fieldwork and logistics. This research benefited early on from enlightened  
790 conversations with Sveta Stuefer and Matthew Sturm. Two anonymous reviewers provided  
791 thoughtful and welcome comments that improved this manuscript. Any use of trade, product, or  
792 firm names is for descriptive purposes only and does not imply endorsement by the US  
793 Government.

794

## 795 **References**

- 796 Armstrong, J. B., Schindler, D. E., Ruff, C. P., Brooks, G. T., Bentley, K. E., and Torgersen, C.  
797 E.: Diel horizontal migration in streams: Juvenile fish exploit spatial heterogeneity in  
798 thermal and trophic resources, *Ecology*, 94, 2066-2075, Doi 10.1890/12-1200.1, 2013.
- 799 Arp, C. D., Schmidt, J. C., Baker, M. A., and Myers, A. K.: Stream geomorphology in a mountain  
800 lake district: hydraulic geometry, sediment sources and sinks, and downstream lake effects,  
801 *Earth Surface Processes and Landforms*, 32, 525-543, Doi 10.1002/Esp.1421, 2007.
- 802 Arp, C., Jones, B., Beck, R., Whitman, M., Derry, J., Lilly, M., and Grosse, G.: Variation in  
803 snow-water equivalent (SWE) among tundra, lakes, and streams on the Alaskan Arctic  
804 Coastal Plain: implications for regional SWE estimates and ice-thickness, Annual  
805 Conference of the American Water Resources Association, Philadelphia, PA, November 2,  
806 2010.
- 807 Arp, C. D., Jones, B. M., Lu, Z., and Whitman, M. S.: Shifting balance of lake ice regimes on the  
808 Arctic Coastal Plain of northern Alaska *Geophysical Research Letters*, 39, 1-5, 2012a.
- 809 Arp, C. D., Whitman, M. S., Jones, B. M., Kemnitz, R., Grosse, G., and Urban, F. E.: Drainage  
810 network structure and hydrologic behavior of three lake-rich watersheds on the Arctic  
811 Coastal Plain, Alaska, *Arctic, Antarctic, and Alpine Research*, 44, 385-398, 2012b.
- 812 Best, H., McNamara, J. P., and Liberty, L.: Association of ice and river channel morphology  
813 determined using ground-penetrating radar in the Kuparuk River, Alaska, *Arctic, Antarctic,  
814 and Alpine Research*, 37, 157-162, 2005.

815 Betts, E., and Kane, D. L.: Understanding the mechanisms by which a perennial Arctic stream  
816 appears intermittent, American Geophysical Union Fall Meeting, San Francisco, 2011.

817 Bowling, L. C., Kane, D. L., Gieck, R. E., Hinzman, L. D., and Lettenmaier, D. P.: The role of  
818 surface storage in a low-gradient Arctic watershed, *Water Resources Research*, 39, 1087,  
819 doi:10.1029/2002WR0010466, 2003.

820 Brewer, M. C.: The thermal regime of an arctic lake, *Transactions of the American Geophysical*  
821 *Union*, 39, 278-284, 1958.

822 Brosten, T. R., Bradford, J. H., McNamara, J. P., Zarnetske, J. P., Gooseff, M. N., and Bowden,  
823 W. B.: Profiles of temporal thaw depths beneath two arctic stream types using ground-  
824 penetrating radar, *Permafrost and Periglacial Processes*, 17, 341-355, 2006.

825 Brown, J.: An estimation of ground ice, coastal plain, northern Alaska, US Army Cold Regions  
826 Research and Engineering Laboratory Hanover, NH, 22, 1968.

827 Brown, J., Ferrians, O. J., Heginbottom, J. A., and Melnikov, E. S.: Circum-arctic map of  
828 permafrost and ground ice conditions, National Snow and Ice Data Center, Boulder, CO,  
829 1998.

830 Burn, C. R.: Tundra lakes and permafrost, Richards Island, western Arctic coast, Canada,  
831 *Canadian Journal of Earth Science*, 39, 1281-1298, doi:10.1139/E02-035, 2002.

832 Carter, L. D.: A Pleistocene sand sea on the Alaskan Arctic coastal plain, *Science*, 211, 381-383,  
833 1981.

834 Carter, L. D., and Galloway, J. P.: Engineering Geologic Map of the Harrison Bay Quadrangle,  
835 Alaska, U.S. Geological Survey, Menlo Park, CA, 2005.

836 Craig, P. C., and McCart, P. J.: Classification of stream types in Beaufort Sea drainages between  
837 Prudhoe Bay, Alaska and the MacKenzie Delta, N.W.T., Canada, *Arctic and Alpine*  
838 *Research*, 7, 183-198, 1975.

839 Crawford, R. H.: Structure of an air-breathing organ and the swim bladder in the Alaska  
840 blackfish, *Dallia pectoralis* Bean, *Canadian Journal of Zoology*, 52, 1221-1225, 1974.

841 Davis, N.: Permafrost: a guide to frozen ground in transition, University of Alaska Press,  
842 Fairbanks, 351 pp., 2001.

843 Ensom, T. P., Burn, C. R., and Kokelj, S. V.: Lake- and channel-bottom temperatures in the  
844 Mackenzie Delta, Northwest Territories, *Can J Earth Sci*, 49, 963-978, Doi 10.1139/E2012-  
845 001, 2012.

846 Frohn, R. C., Hinkel, K. M., and Eisner, W. R.: Satellite remote sensing classification of thaw  
847 lakes and drained thaw lake basins on the North Slope of Alaska, *Remote Sensing of*  
848 *Environment*, 97, 116-126, DOI 10.1016/j.rse.2005.04.022, 2005.

849 Grosse, G., Jones, B. and Arp, C.: Thermokarst Lakes, Drainage, and Drained Basins, in: *Treatise*  
850 *on Geomorphology*, edited by: Schroder, J., Giardino, R., and Harbor, J., Academic Press,  
851 San Diego, 1-29, 2013.

852 Heim, K.: *Seasonal Movements of Arctic Grayling in a Small Stream on the Arctic Coastal Plain,*  
853 *Alaska*, M.S., School of Fisheries and Ocean Sciences, University of Alaska Fairbanks,  
854 Fairbanks, 2014.

855 Hinkel, K. M., Frohn, R. C., Nelson, F. E., Eisner, W. R., and Beck, R. A.: Morphometric and  
856 spatial analysis of thaw lakes and drained thaw lake basins in the western Arctic Coastal  
857 Plain, Alaska, *Permafrost and Periglacial Processes*, 16, 327-341, 2005.

858 Jones, B. M., Arp, C. D., Hinkel, K. M., Beck, R. A., Schmutz, J. A., and Winston, B.: Arctic  
859 lake physical processes and regimes with implications for winter water availability and  
860 management in the National Petroleum Reserve Alaska, *Environmental Management*, 43,  
861 1071-1084, 10.1007/s00267-008-9241-0, 2009a.

862 Jones, B. M., Kolden, C. A., Jandt, R., Abatzoglou, J. T., Urban, F., and Arp, C. D.: Fire  
863 Behavior, Weather, and Burn Severity of the 2007 Anaktuvuk River Tundra Fire, North  
864 Slope, Alaska, *Arct Antarct Alp Res*, 41, 309-316, Doi 10.1657/1938-4246-41.3.309,  
865 2009b.

866 Jones, B. M., Gusmeroli, A., Arp, C. D., Strozzi, T., Grosse, G., Gaglioti, B. V., and Whitman,  
867 M. S.: Classification of freshwater ice conditions on the Alaskan Arctic Coastal Plain using  
868 ground penetrating radar and TerraSAR-X satellite data, *International Journal of Remote*  
869 *Sensing*, 34, 8267-8279, Doi 10.1080/2150704x.2013.834392, 2013.

870 Jones, N. E.: Incorporating lakes within the river discontinuum: longitudinal changes in  
871 ecological characteristics in stream-lake networks, *Canadian Journal of Fisheries and*  
872 *Aquatic Sciences*, 67, 1350-1362, Doi 10.1139/F10-069, 2010.

873 Jorgenson, M. T., Shur, Y. L., and Pullman, E. R.: Abrupt increase in permafrost degradation in  
874 Arctic Alaska, *Geophysical Research Letters*, 33, 1-4, 2006.

875 Jorgenson, M. T., and Shur, Y.: Evolution of lakes and basins in northern Alaska and discussion  
876 of the thaw lake cycle, *Journal of Geophysical Research*, 112, 1-12,  
877 doi:10.1029/2006JF000531, 2007.

878 Jorgenson, M. T., Romonovsky, V., Yoshikawa, K., Kanevskiy, M., Shur, Y., Marchenko, S.,  
879 Brown, J., and Jones, B.: Permafrost characteristics of Alaska - a new permafrost map of  
880 Alaska, Ninth International Conference on Permafrost, Fairbanks, AK, 2008.

881 Kanevskiy, M., Shur, Y., Jorgenson, M. T., Ping, C-L., Michaelson, G. J., Fortier, D., Stephani,  
882 E., Dillon, M., and Tumskoy, V.: Ground ice in the upper permafrost of the Beaufort Sea  
883 coast of Alaska, *Cold Regions Science and Technology*, 85, 56-70, 2013.

884 Lachenbruch, A. H., Brewer, M. C., Greene, G. W., and Marshall, B. V.: Temperatures in  
885 permafrost, in: *Temperature, its Measurement and Control in Science and Industry*, 791-  
886 803, 1962.

887 Lachenbruch, A. H.: Contraction theory of ice-wedge polygons: a qualitative discussion,  
888 Permafrost International Conference, Lafayette, Indiana, 1966, 63-70,

889 Manley, W. F., and Kaufman, D. S.: *Alaska PaleoGlacier Atlas*, Institute of Arctic and Alpine  
890 Research (INSTAAR), University of Colorado, Boulder, CO, 2002.

891 McFarland, J., M. W. Wipfli, and M. S. Whitman: Feeding ecology of Arctic grayling in a small  
892 beaded stream on the Arctic Coastal Plain, Alaska, Conference of the Alaska Chapter of the  
893 American Fisheries Society, Kodiak, AK, Oct. 23, 2012.

894 McKnight, D. M., Gooseff, M. N., Vincent, W. F., and Peterson, B. J.: High-latitude rivers and  
895 streams, in: *Polar Rivers and Lakes*, edited by: Vincent, W. F., and Laybourn-Parry, J.,  
896 Oxford University Press, Oxford, 83-102, 2008.

897 McNamara, J. P., Kane, D. L., and Hinzman, L. D.: An analysis of an arctic channel network  
898 using a digital elevation model, *Geomorphology*, 29, 339-353, 1999.

899 Merck, M. F., and Neilson, B. T.: Modelling in-pool temperature variability in a beaded arctic  
900 stream, *Hydrological Processes*, 26, 3921-3933, Doi 10.1002/Hyp.8419, 2012.

901 Merck, M. F., Neilson, B. T., Cory, R. M., and Kling, G. W.: Variability of in-stream and riparian  
902 storage in a beaded arctic stream, *Hydrological Processes*, 26, 2938-2950, Doi  
903 10.1002/Hyp.8323, 2012.

904 Montgomery, D. R., and Dietrich, W. E.: Source areas, drainage density, and channel initiation,  
905 *Water Resources Research*, 25, 1907-1918, 1989.



906 Montgomery, D. R., and Buffington, J. M.: Channel-reach morphology in mountain drainage  
907 basins, *Geological Society of America Bulletin*, 109, 596-611, 1997.

908 Oswood, M. W., Everett, K. R., and Schell, D. M.: Some physical and chemical characteristics of  
909 an arctic beaded stream, *Holarctic Ecology*, 12, 290-295, 1989.

910 Pewé, T. L.: Ice-wedges in Alaska - classification, distribution, and climatic significance,  
911 *Permafrost International Conference*, Lafayette, Indiana, 1966, 76-81,

912 Reimer, P. J., Bard, E., Bayliss, A., Beck, J. W., Blackwell, P. G., Ramsey, C. B., Buck, C. E.,  
913 Cheng, H., Edwards, R. L., Friedrich, M., Grootes, P. M., Guilderson, T. P., Haflidason, H.,  
914 Hajdas, I., Hatte, C., Heaton, T. J., Hoffmann, D. L., Hogg, A. G., Hughen, K. A., Kaiser,  
915 K. F., Kromer, B., Manning, S. W., Niu, M., Reimer, R. W., Richards, D. A., Scott, E. M.,  
916 Southon, J. R., Staff, R. A., Turney, C. S. M., and van der Plicht, J.: Intcal13 and Marine13  
917 Radiocarbon Age Calibration Curves 0-50,000 Years Cal Bp, *Radiocarbon*, 55, 1869-1887,  
918 2013.

919 Rosgen, D. L.: A classification of natural rivers, *Catena*, 22, 169-199, 1994.

920 Runkel, R. L.: Using OTIS to model solute transport in streams and rivers, USGS, Denver, CO,  
921 *Fact Sheet FS-138-99*, 1-4, 2000.

922 Scott, K. M.: Effects of permafrost on stream channel behavior in Arctic Alaska, USGS,  
923 Washington, D.C., *Geological Survey Professional Paper 1068*, 1-19, 1978. Scott, W. B., and  
924 Crossman, E. J.: *Freshwater fishes of Canada*, Fisheries Research Board of Canada, 1973.

925 Sturm, M., Racine, C., and Tape, K.: Increasing shrub abundance in the Arctic, *Nature*, 411, 546-  
926 547, 2001.

927 Tarbeeveva, A. M., and Surkov, V. V.: Beaded channels of small rivers in permafrost zones,  
928 *Geography and Natural Resources*, 34, 27-32, 10.1134/S18753728130300439, 2013.

929 Vasudevan, D., Fimmen, R. L., and Francisco, A. B.: Tracer-grade rhodamine WT: structure of  
930 constituent isomers and their sorption behavior, *Environmental Science and Technology*,  
931 35, 4089-4096, 2001.

932 West, R. L., Smith, M. W., Barber, W. E., Reynolds, J. B., and Hop, H.: Autumn Migration and  
933 Overwintering of Arctic Grayling in Coastal Streams of the Arctic National Wildlife  
934 Refuge, Alaska, *Transactions of the American Fisheries Society*, 121, 709-715, Doi  
935 10.1577/1548-8659(1992)121<0709:Amaooa>2.3.Co;2, 1992.

936 Whiting, P. J., and Bradley, J. B.: A process-based classification system for headwater streams,  
937 Earth Processes and Landforms, 18, 603-612, 1993.

938 Wohl, E.: Mountain Rivers, Water Resources Monograph 14, American Geophysical Union,  
939 Washington, D.C., 320 pp., 2000.

940 Woo, M.: Permafrost Hydrology, Springer-Verlag, New York, 563 pp., 2012.

941 Zarnetske, J. P., Gooseff, M. N., Brosten, T. R., Bradford, J. H., McNamara, J. P., and Bowden,  
942 W. B.: Transient storage as a function of geomorphology, discharge, and permafrost active  
943 layer conditions in Arctic tundra streams, Water Resources Research, 43, 1-13,  
944 10.1029/2005WR004816, 2007.

945 Zarnetske, J. P., Gooseff, M. N., Bowden, W. B., Greenwald, M. J., Brosten, T. R., Bradford, J.  
946 H., and McNamara, J. P.: Influence of morphology and permafrost dynamics on hyporheic  
947 exchange in arctic headwater streams under warming climate conditions, Geophysical  
948 Research Letters, 35, 1-5, 10.1029/2007GL032049, 2008.

949

936 Whiting, P. J., and Bradley, J. B.: A process-based classification system for headwater streams,  
937 Earth Processes and Landforms, 18, 603-612, 1993.

938 Wohl, E.: Mountain Rivers, Water Resources Monograph 14, American Geophysical Union,  
939 Washington, D.C., 320 pp., 2000.

940 Woo, M.: Permafrost Hydrology, Springer-Verlag, New York, 563 pp., 2012.

941 Zarnetske, J. P., Gooseff, M. N., Brosten, T. R., Bradford, J. H., McNamara, J. P., and Bowden,  
942 W. B.: Transient storage as a function of geomorphology, discharge, and permafrost active  
943 layer conditions in Arctic tundra streams, Water Resources Research, 43, 1-13,  
944 10.1029/2005WR004816, 2007.

945 Zarnetske, J. P., Gooseff, M. N., Bowden, W. B., Greenwald, M. J., Brosten, T. R., Bradford, J.  
946 H., and McNamara, J. P.: Influence of morphology and permafrost dynamics on hyporheic  
947 exchange in arctic headwater streams under warming climate conditions, Geophysical  
948 Research Letters, 35, 1-5, 10.1029/2007GL032049, 2008.

949

Table 1. Summary of a Circum-Arctic inventory of beaded stream networks in the zone of continuous permafrost based on a survey of high resolution (<5-m, summer) imagery available in Google Earth™ during 2012-13. The relative proportion of high resolution imagery available in each region was used to estimate the total number of stream networks and drainage density assuming an average network length of 10 km.

<b>Region</b>	<b>Area (km<sup>2</sup>)</b>	<b>% Area with High Resolution Imagery (snow-free)</b>	<b>Identified Stream Networks</b>	<b>Estimated Stream Networks</b>	<b>Estimated Drainage Density (km/km<sup>2</sup>)</b>
Northern Canada	2,347,072	9	22	244	0.001
Northern Alaska (U.S.A)	185,907	80	275	344	0.019
Northern Russia	2,123,067	11	148	1346	0.006

Table 2. Comparison of beaded stream morphology and ambient thermokarst features between black and white photography acquired in 1948 and color infrared photography acquired in 2013 for a 2.7 km segment of Crea Creek in the lower Fish Creek Watershed.

<b>Attribute Compared</b>	<b>1948</b>	<b>2013</b>
<b>Pools</b>		
number	132	134
total area (m <sup>2</sup> )	7,861	8,334
mean area (m <sup>2</sup> )	59.6	62.2
number unique	23	25
<b>Gulch / Riparian Zone</b>		
total area (m <sup>2</sup> )	221,802	241,247
mean width (m)	82.1	89.4
<b>Thaw pits</b>		
total number	74	66
number unique	55	47

Table 3. Results from reach-scale tracer injections for Crea (325 m, shallow elliptical beads) and Blackfish (232 m, deep coalesced beads) creeks during the summer of 2013 (RWT is rhodamine WT, Q is stream discharge, A is the advective cross-sectional area, U is advective zone velocity, D is the dispersion coefficient, A<sub>S</sub> is the storage zone cross-sectional area, A<sub>S</sub>/A is the relative storage zone area, α is the storage zone exchange coefficient, A<sub>R</sub> and U<sub>R</sub> are the cross-sectional area and velocity, respectively, of a single channel run). Comparisons of these results are made to two other RWT tracer studies of similar sized stream with beaded and other channel morphologies.

Experiment Data			Total Channel Hydraulics				Channel Storage Zone			Channel Run (single)	
Site	Date	Solute Added (RWT, g)	Q (m <sup>3</sup> /s)	A (m <sup>2</sup> )	U (m/s)	D (m <sup>2</sup> /s)	A <sub>S</sub> (m <sup>2</sup> )	A <sub>S</sub> /A	α (s <sup>-1</sup> )	A <sub>R</sub> (m <sup>2</sup> )	U <sub>R</sub> (m/s)
<u>beaded streams in Fish Creek Watershed in 2013 (this study)</u>											
<b>Crea</b>	14-Jun	70.4	1.17	5.29	0.22	3.33	5.32	1.01	1.9E-03	2.48	0.54
<b>Crea</b>	5-Jul	49.9	0.13	1.89	0.04	0.88	2.71	1.43	5.9E-04	0.43	0.39
<b>Crea</b>	25-Aug	19.9	0.03	1.95	0.01	0.38	2.55	1.31	1.2E-03	0.10	0.33
<b>Blackfish</b>	13-Jun	92.4	1.73	9.81	0.18	1.90	9.08	0.93	3.2E-03	2.90	0.70
<b>Blackfish</b>	6-Jul	41.4	0.09	7.00	0.01	0.45	6.60	0.94	1.5E-03	0.52	0.33
<b>Blackfish</b>	24-Aug	19.1	0.03	-	-	-	-	-	-	0.36	0.15
<u>multiple stream types near Toolik Lake in 2004 (Zarnetske et al., 2007)</u>											
<b>Lake inlet</b>	17-Jun	-	0.26	-	0.16	1.48	-	-	2.0E-4	-	-
<b>Lake outlet</b>	18-Jun	-	0.09	-	0.07	1.71	-	-	5.0E-4	-	-
<b>Beaded</b>	25-Jun	-	0.05	-	0.02	1.75	-	-	3.0E-4	-	-
<b>Beaded</b>	21-Jun	-	0.44	-	0.09	1.94	-	-	6.0E-4	-	-
<u>multiple stream types in a mountain meadow in 2004 (Arp unpublished data, streams described in Arp et al., 2007)</u>											
<b>Alluvial</b>	11-Aug	-	0.14	-	0.22	-	-	0.69	1.6E-4	-	-
<b>Lake outlet</b>	10-Aug	-	0.17	-	0.06	-	-	0.23	6.7E-4	-	-

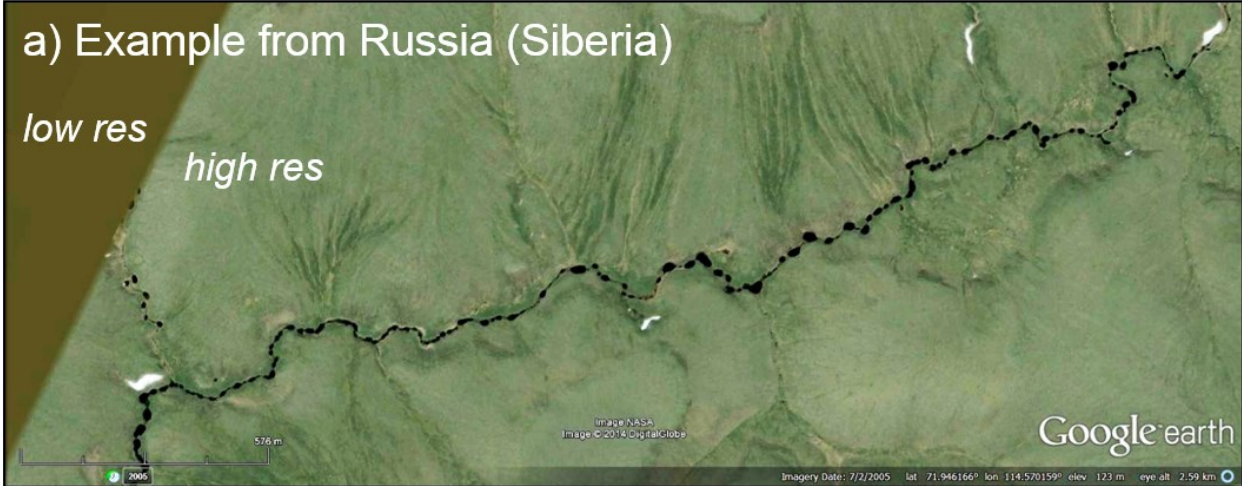


Figure 1. Examples of beaded stream networks located by scanning high resolution (< 5-m) imagery available in Google Earth in a) Russia (Anabar River Watershed), b) U.S.A (near Nuiqsut, Alaska), and c) Canada (Tuktoyaktuk Peninsula).

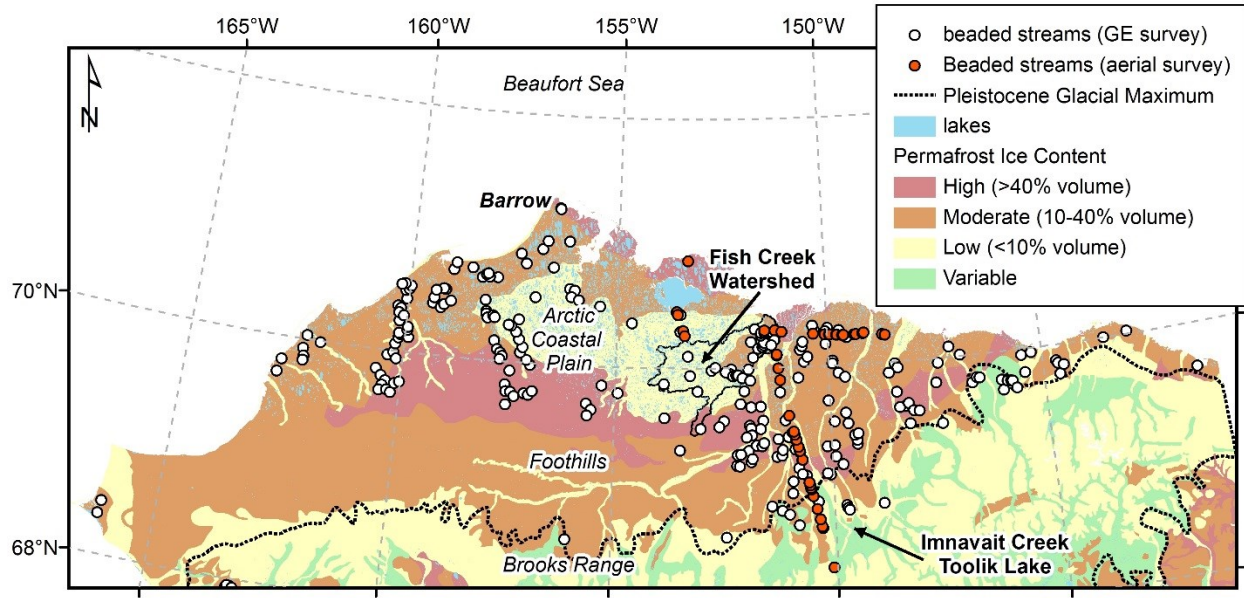


Figure 2. The distribution of beaded streams located using Google Earth and from aerial surveys across the North Slope of Alaska in relation to permafrost ice content (Jorgenson et al. 2008) and the Pleistocene glacial maximum (Manley and Kaufman 2002). The locations of Fish Creek Watershed (focus area of this study) and Innavait Creek (focus area of the majority of previous work on beaded streams) are indicated.



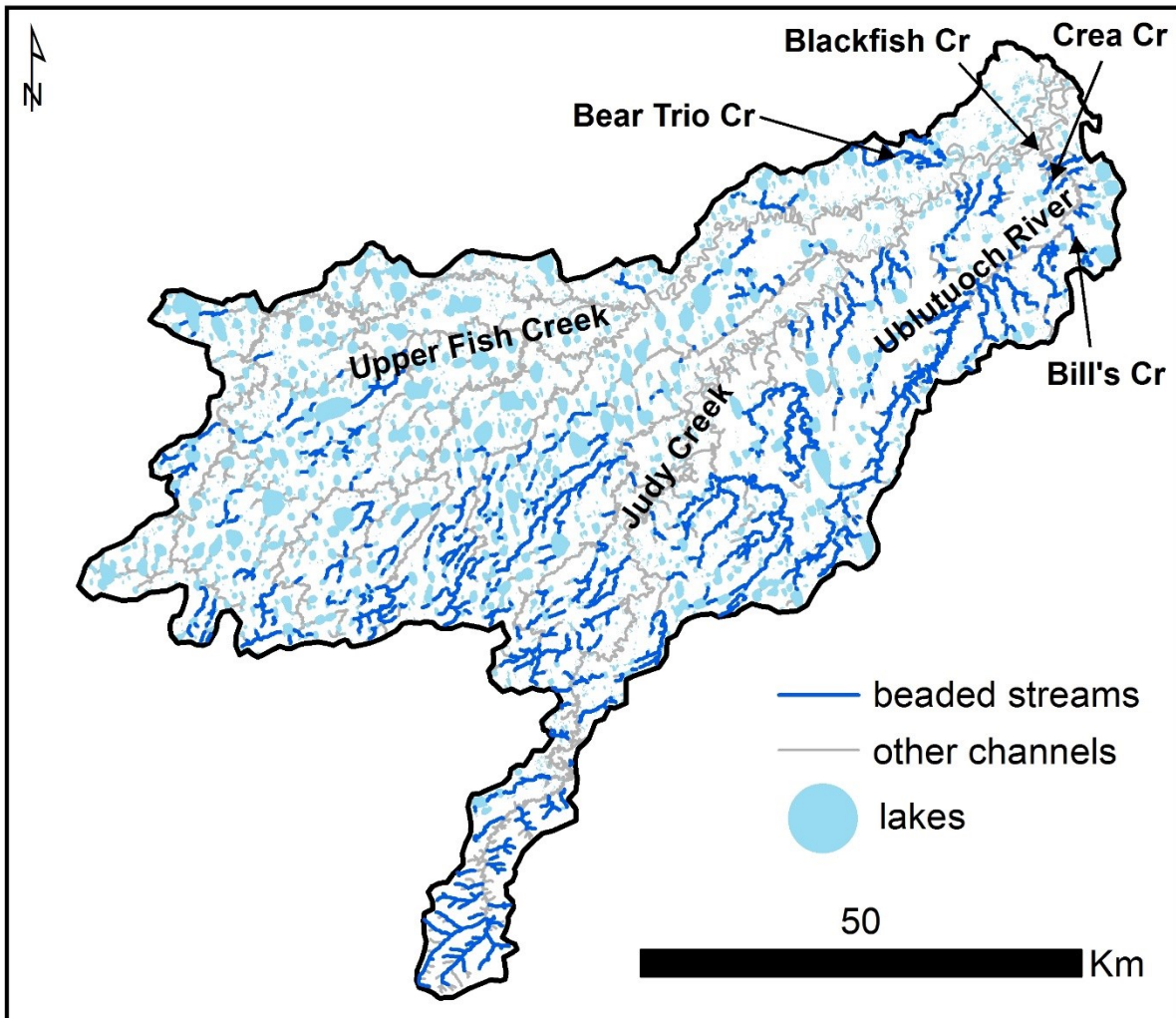


Figure 3. The drainage network of Fish Creek Watershed (location shown in Fig. 2) showing all beaded stream networks that were delineated from 2.5-m CIR photography. River systems and individual beaded stream catchments where more detailed field and geospatial studies were conducted for this study are indicated.

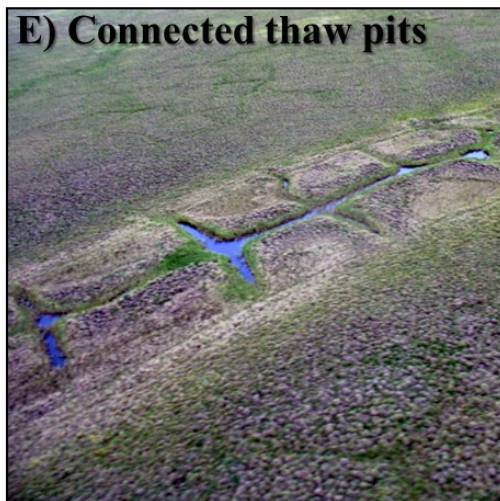
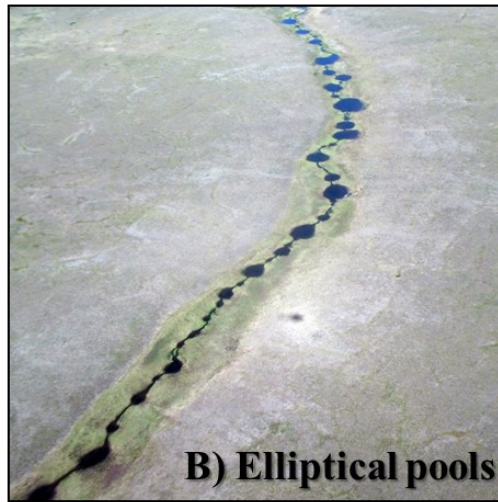


Figure 4. Oblique photographs showing typical pool-run morphology (A) and examples of beaded channels forms (B-E) compared to alluvial channel (F) morphology.

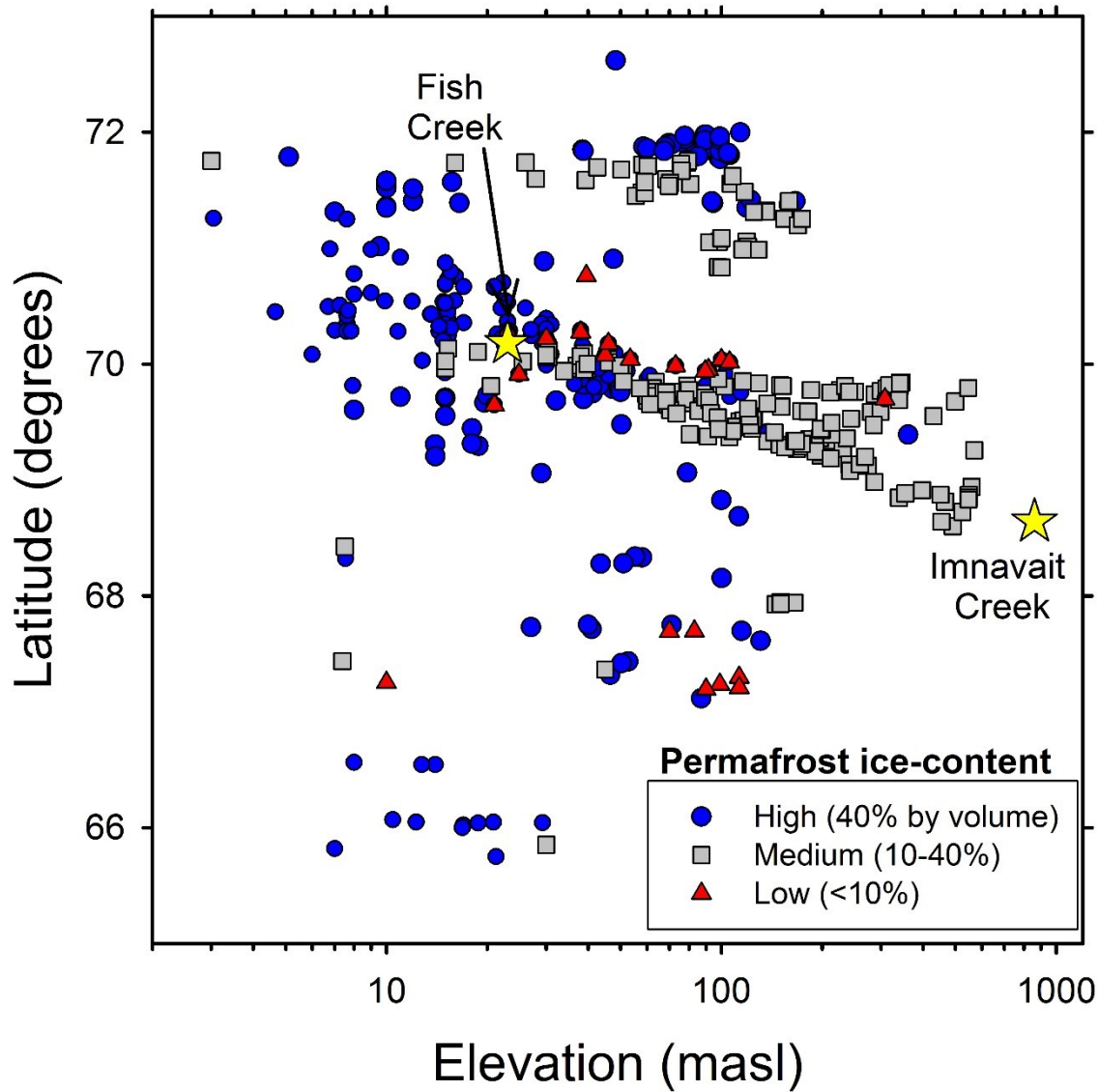


Figure 5. The distribution of beaded stream channels throughout the circumarctic in relation to latitude, elevation, and permafrost ground-ice content. Stream networks were identified using imagery in Google Earth in the zone of continuous permafrost where high resolution imagery was available. The location of streams in the Fish Creek (focus area for this study) and Imnavait Creek (focus area for majority of previous beaded stream research) are indicated with yellow stars.

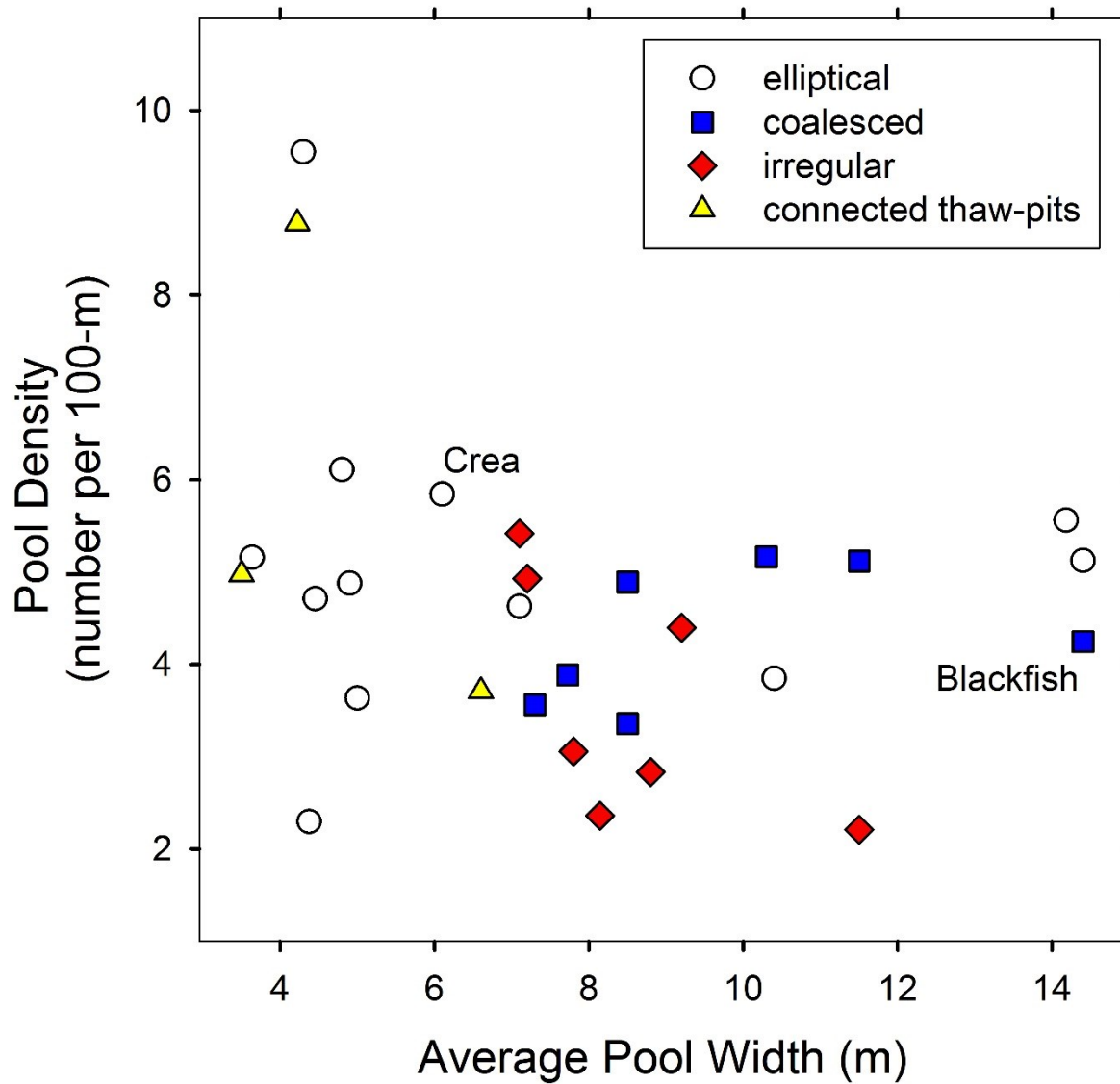


Figure 6. Morphological characteristics of beaded streams compared according to pool (bead) density, size, and shape classes (examples shown in Fig. 4 and locations shown in Fig. 3) at the segment scale (1 – 3 km channel length) in the Fish Creek Watershed.

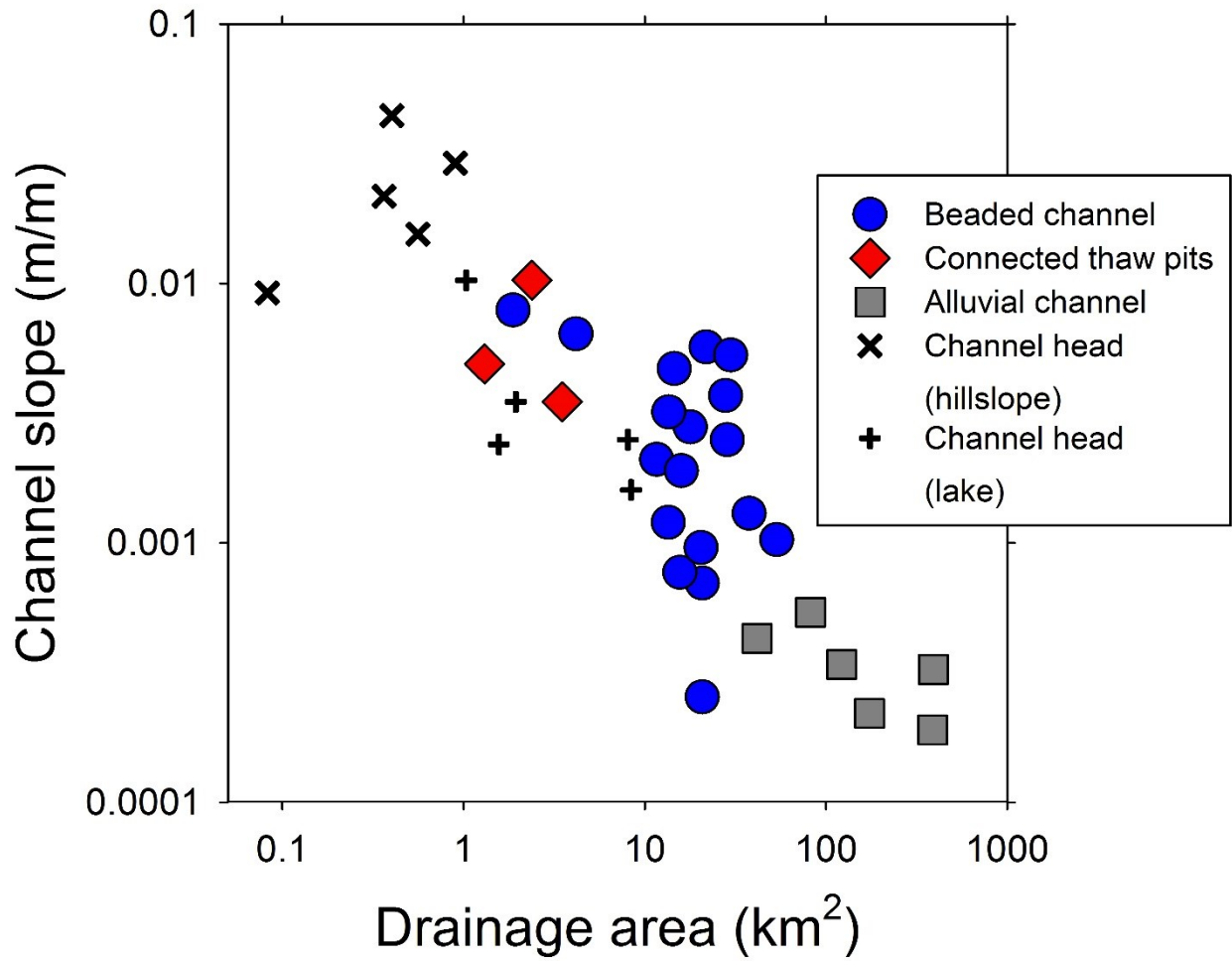


Figure 7. The organization of the major channel forms and channel initiation points (heads) in the Fish Creek Watershed are shown in relation to drainage area and channel slope (measured from a 5-m DEM).

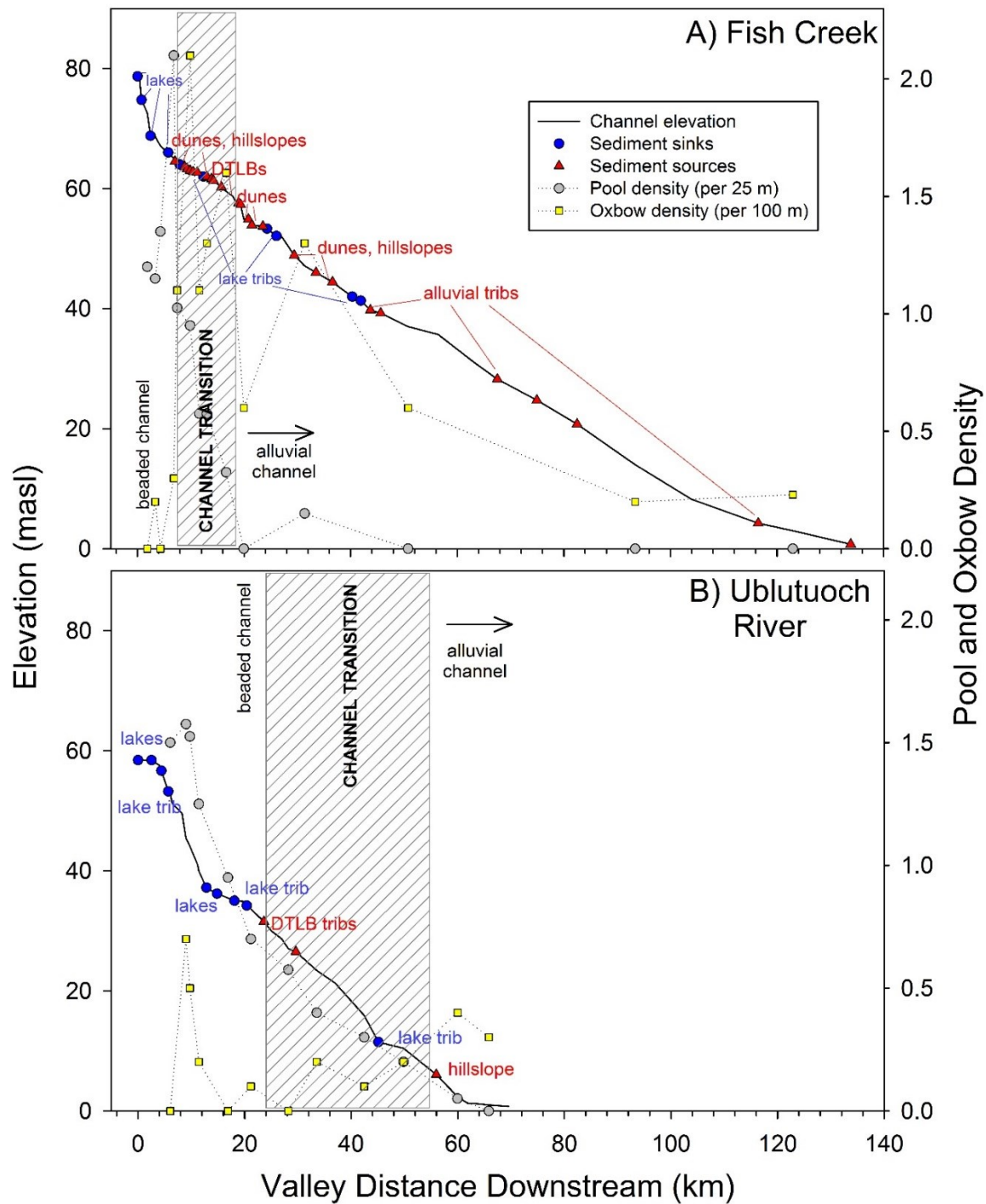


Figure 8. Headwater to downstream patterns of a beaded stream originating in the eolian sand deposits, Fish Creek (A), compared with a beaded stream originating in alluvial-marine deposits, Ublutuoch River (B) showing changes in channel elevation and the density of pools and oxbow (meander-cutoff) lakes relative to sediment sources and sinks.

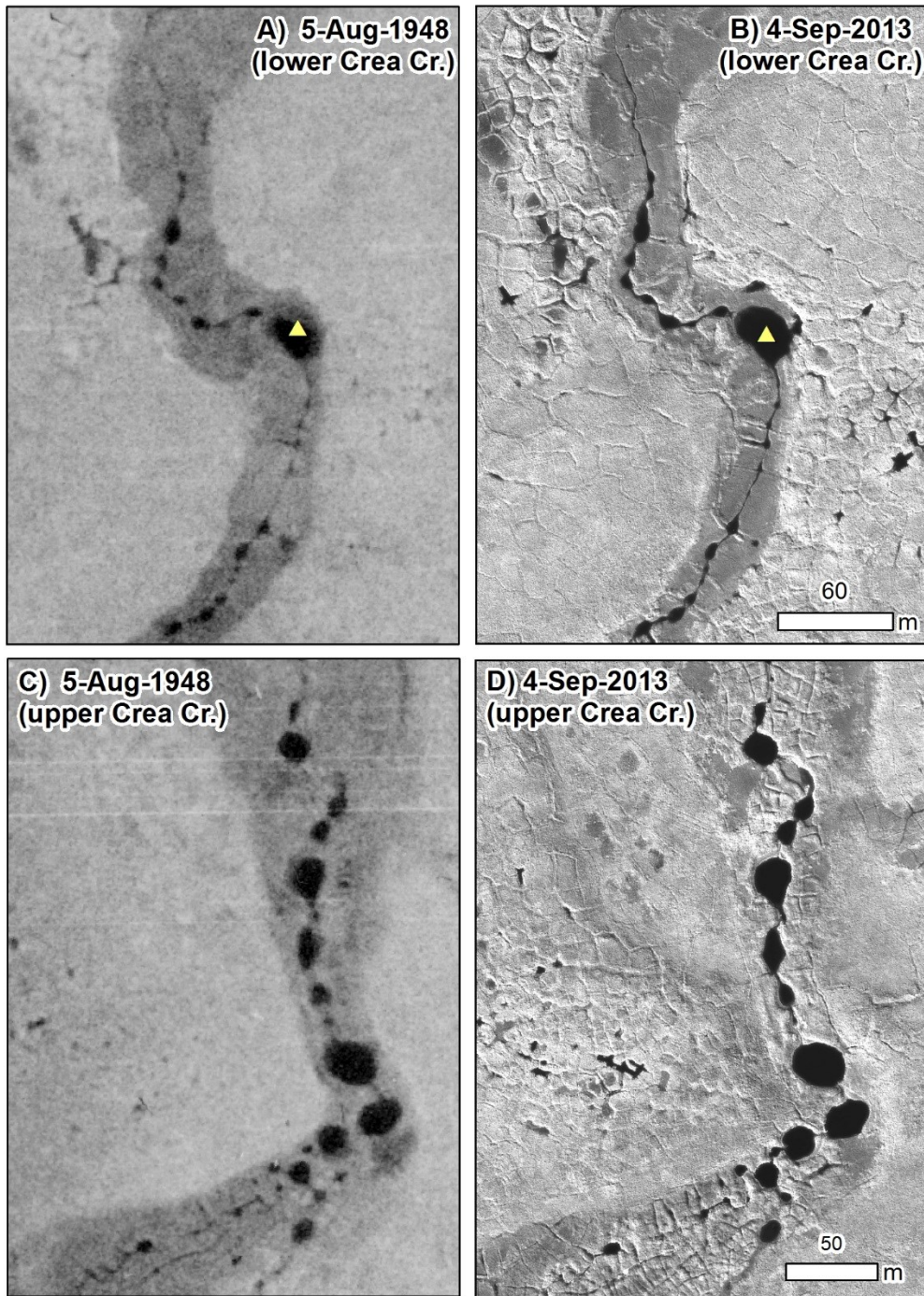


Figure 9. Comparison of two segments of the Crea Creek channel in 1948 (A, C) and 2013 (B, D) showing that pools, the riparian gulch, and adjacent thaw pits can be clearly observed in each image. The location of a sediment core collected for  $^{14}\text{C}$  dating is indicated with a yellow triangle (location of Crea Creek is shown in Fig. 3).

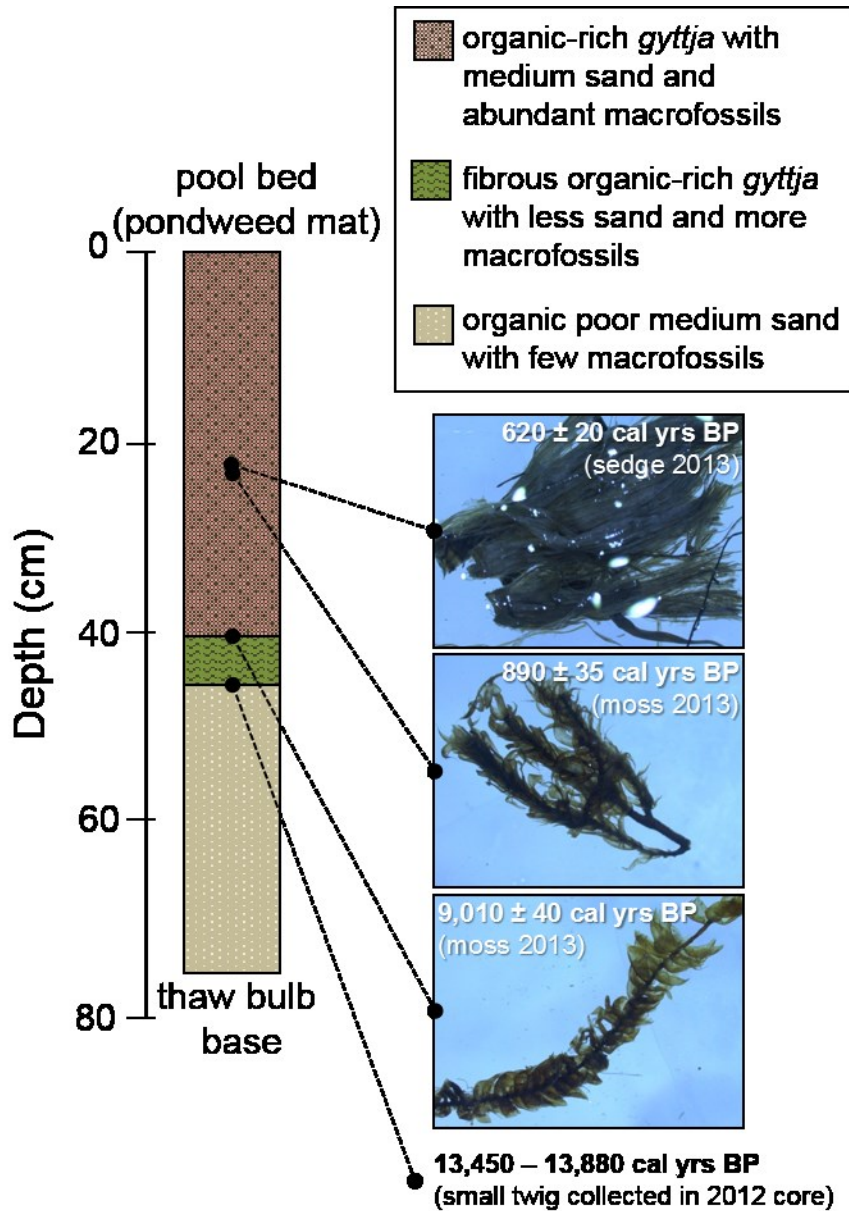


Figure 10. Diagram of generalized sediment core stratigraphy from a large pool in Crea Creek (indicated in Fig. 9) collected in both 2012 and 2013 showing location of macrofossil fragments collected for radiocarbon dating. The sharp transition from organic-rich *gyttja* to medium sand is interpreted to be the base of the pool at its time of formation.



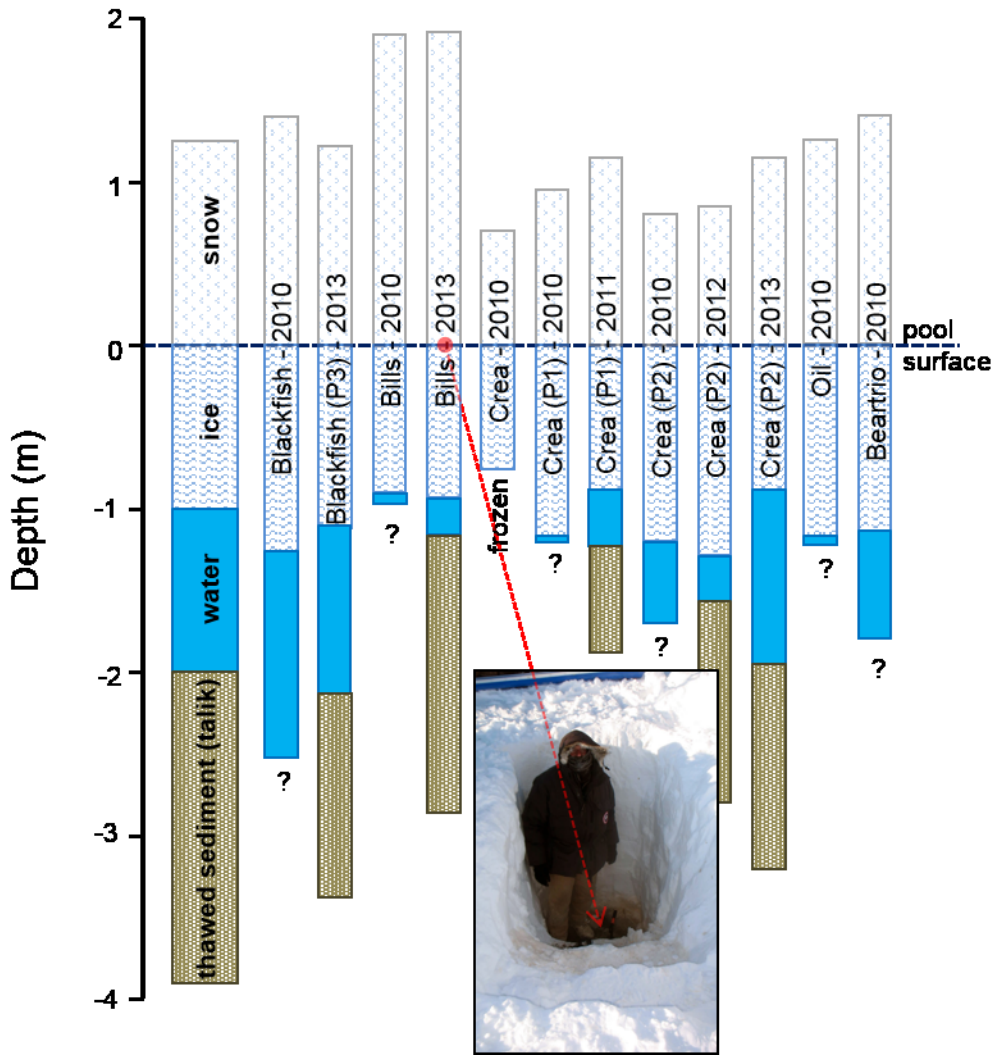


Figure 11. Late winter profiles (March or April) of several pools (beads) surveyed in multiple beaded streams from 2010 to 2013 (“?” indicated that no measurement of thawed sediment depth was attempted). An example photograph from one pool surveyed in 2013 shows a 1.9-m tall person (G. Grosse) standing on the frozen pool surface for scale.

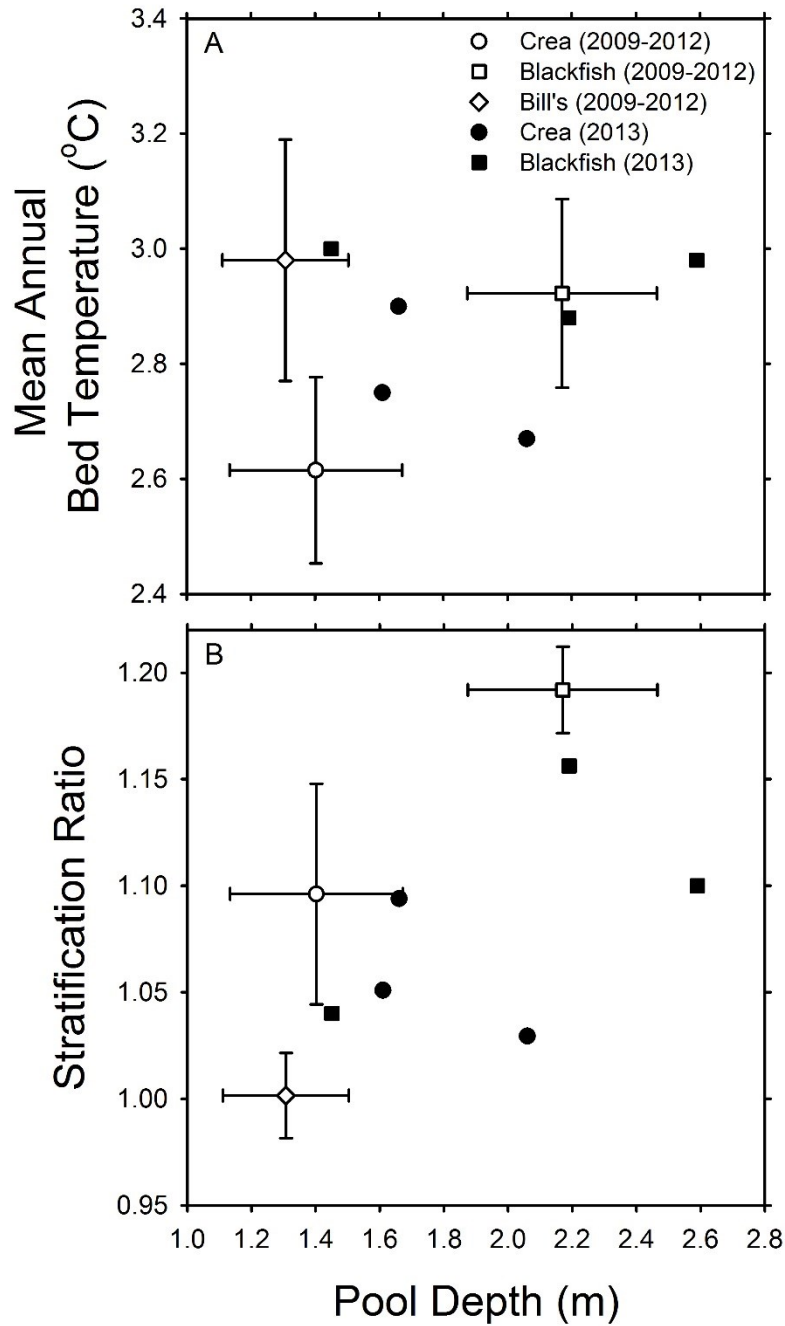


Figure 12. Thermal regime characteristics of single pools at three beaded streams averaged over four years (error bars are standard deviations). In 2013, three additional pools within two of these beaded streams were monitored to assess within-stream variability of thermal characteristics. Thermal regimes were characterized by mean annual temperatures at pool beds (A) and stratification ratios as the average ratio between the pool surface and bed during the period from July to mid-August in each year (B). Pool depths are averaged during the same period that temperature was summarized in each plot.

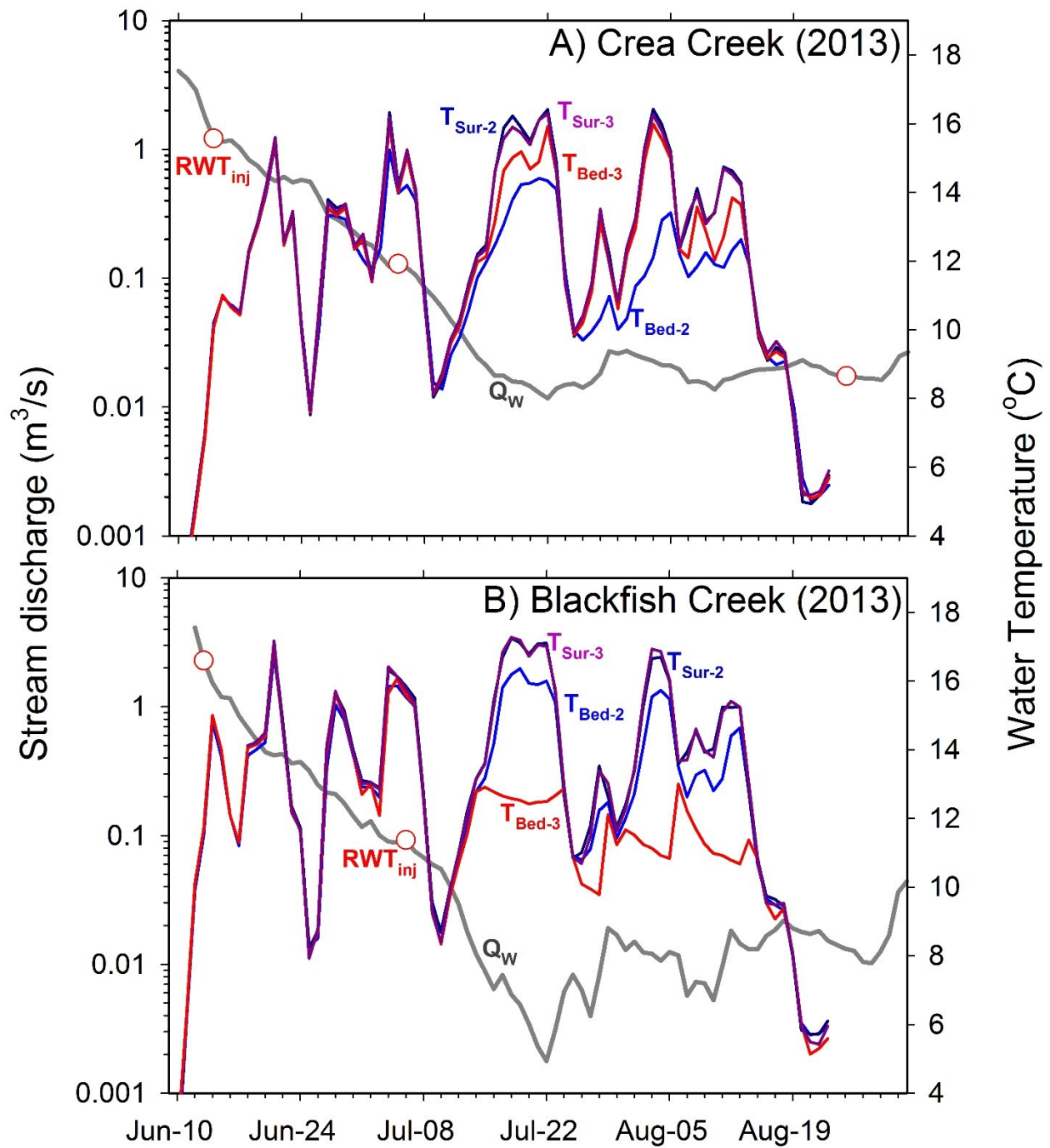


Figure 13. Streamflow hydrographs and temperature regimes for two beaded streams (Crea (A) and Blackfish (B) creeks) with contrasting channel and watershed morphology. Bed and surface temperatures were monitored in multiple pools within each reach to document the timing, magnitude, and variation in stratification in relation to streamflow (streamflow is indicated by  $Q_w$ , temperatures are indicated at pool beds by  $T_{bed}$  and pool surface by  $T_{sur}$ , and timing of water tracer injections studies are indicated with red circles by  $RWT_{inj}$ ; all data are presented as mean daily values from hourly measurements).

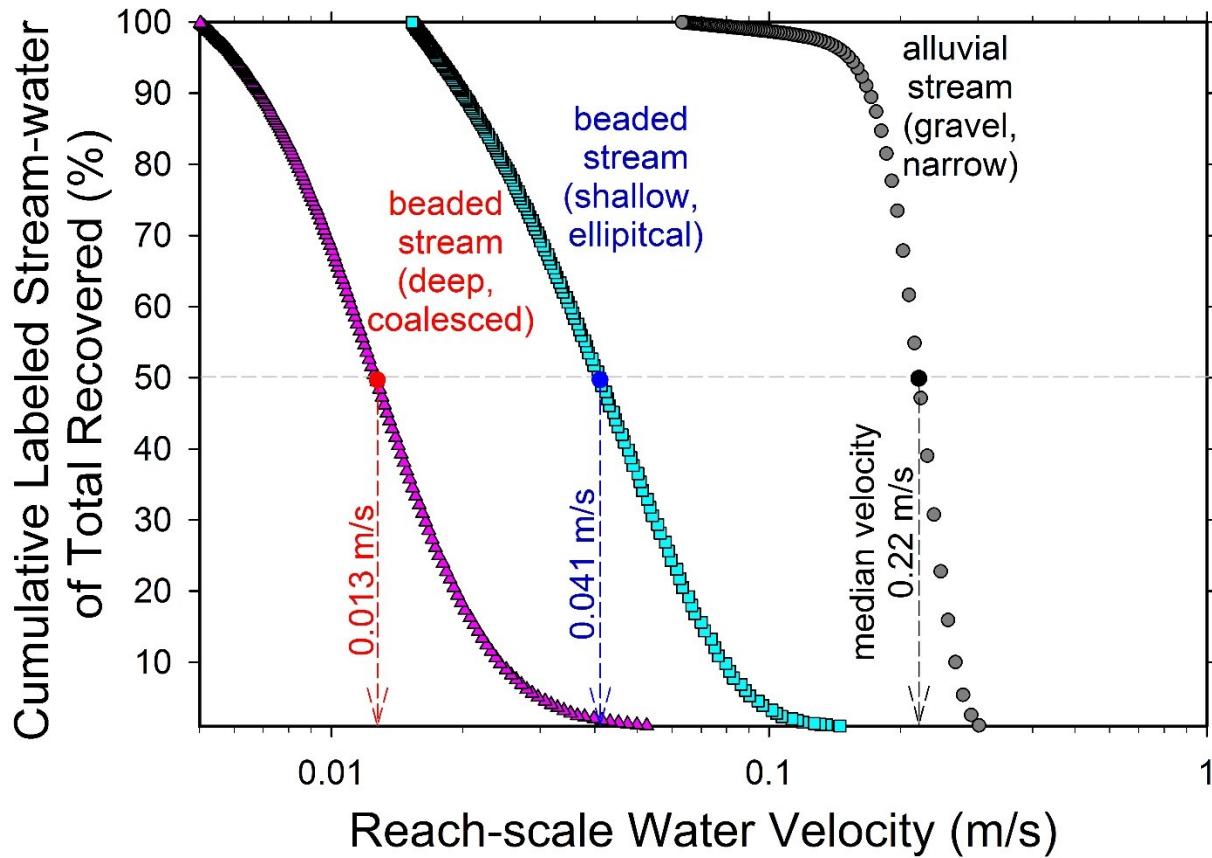


Figure 14. Examples of reach-scale water velocity distributions (reach length / travel time) measured using hydrologic tracer tests (rhodamine WT pulse additions) shown as cumulative tracer recovered downstream. Results from two beaded streams, Crea Creek (blue squares) and Blackfish Creek (red triangles) are compared to an alluvial stream (black circles) in a mountain meadow (Arp unpublished data, stream described in Arp et al. 2007); all three streams had similar discharges ranging from 85-140 L/s during tracer tests and slopes ranging from 0.1-0.2 %, but with otherwise differing morphologies (experimental data and inverse modeling results shown in Table 3).

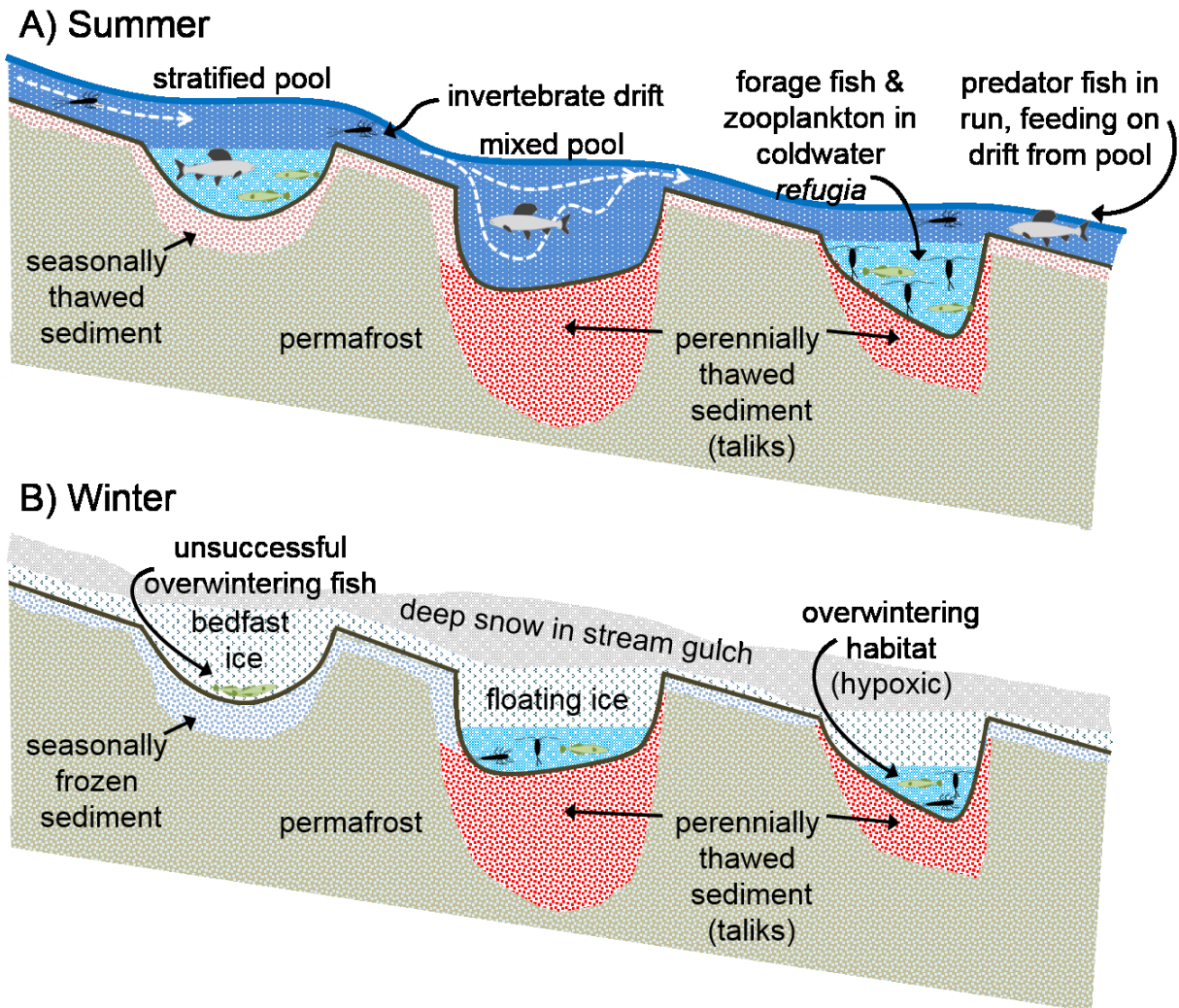


Figure 15. Conceptual diagram showing morphology, physical regimes, habitats, and organisms of a hypothetical pool-run system in the summer (A) and winter (B) based on observations and monitoring studies in multiple beaded stream systems during these time periods over many years.